Inorg. Chem. **2002**, *41*, 2109–2123

Organic–Inorganic Hybrid Materials: Hydrothermal Syntheses and Structural Characterization of Bimetallic Organophosphonate Oxides of the Type Mo/Cu/O/RPO_3^{2-}/Organoimine

Robert C. Finn, Randy S. Rarig, Jr., and Jon Zubieta*

Department of Chemistry, Syracuse University, Syracuse, New York 13244-4100

Received October 31, 2001

The hydrothermal reactions of a Cu(II) starting material, a molybdate source, 2,2′-bipyridine or terpyridine, and the appropriate alkyldiphosphonate ligand yield two series of bimetallic organophosphonate hybrid materials of the general types $[Cu_n(bpy)_mMo_xO_y(H_2O)_p\{O_3P(CH_2)_nPO_3\}_z]$ and $[Cu_n(terpy)_mMo_xO_y(H_2O)_p\{O_3P(CH_2)_nPO_3\}_z]$. The bipyridyl series includes the one-dimensional materials $[Cu(bpy)(MoO_2)(H_2O)(O_3PCH_2PO_3)]$ (**1**) and $[\{Cu(bpy)_2\}\{Cu(bpy)(H_2O)\}(Mo_5O_{15})(O_3PCH_2CH_2CH_2CH_2PO_3)]\cdot H_2O$ (**5**·H_2O) and the two-dimensional hybrids $[Cu(bpy)(Mo_2O_5)(H_2O)(O_3PCH_2PO_3)]\cdot H_2O$ (**2**·H_2O), $[\{Cu(bpy)\}_2(Mo_4O_{12})(H_2O)_2(O_3PCH_2CH_2PO_3)]\cdot 2H_2O$ (**3**·$2H_2O$), and $[Cu(bpy)(Mo_2O_5)(O_3PCH_2CH_2CH_2PO_3)]$(**4**). The terpyridyl series is represented by the one-dimensional $[\{Cu(terpy)(H_2O)\}_2(Mo_5O_{15})(O_3PCH_2CH_2PO_3)]\cdot 3H_2O$ (**7**·$3H_2O$) and the two-dimensional composite materials $[Cu(terpy)(Mo_2O_5)(O_3PCH_2PO_3)]$ (**6**) and $[\{Cu(terpy)\}_2(Mo_5O_{15})(O_3PCH_2CH_2CH_2PO_3)]$ (**8**). The structures exhibit a variety of molybdate building blocks including isolated $\{MoO_6\}$ octahedra in **1**, binuclear subunits in **2**, **4**, and **6**, tetranuclear embedded clusters in **3**, and the prototypical $\{Mo_5O_{15}(O_3PR)_2\}^{4-}$ cluster type in **5**, **7**, and **8**. These latter materials exemplify the building block approach to the preparation of extended structures.

The impressive diversity of compositions,[1] structures,[2] physical properties,[3] and applications[4−27] associated with inorganic oxide solids has stimulated widespread interest in the design of new materials of this family. However, advances in the synthetic inorganic chemistry of solids are often hampered by the lack of suitable soluble molecular building blocks and well-defined reaction chemistries which allow low temperature assembly into crystalline inorganic materials.[28,29]

A number of strategies have been developed in recent years to address the manipulation of oxide structures and the design

* To whom correspondence should be addressed. E-mail: jazubiet@syr.edu. Fax: 315-443-4070.

(1) Greenwood, N. N.; Earnshaw, A. *Chemistry of the Elements*; Pergamon Press: New York, 1984.
(2) Wells, A. F. *Structural Inorganic Chemistry*, 4th ed.; Oxford University Press: Oxford, 1978.
(3) Cheetham, A. J. *Science* **1994**, *264*, 794.
(4) Reynolds, T. G.; Buchanan, R. C. *Ceramic Materials for Electronics*, 2nd ed.; Dekker: New York, 1991, p 207.
(5) Büchner, W.; Schliebs, R.; Winter, G.; Büchel, K. H. *Industrial Inorganic Chemistry*; VCH: New York, 1989.
(6) McCarroll, W. H. *Encyclopedia of Inorganic Chemistry*; John Wiley and Sons: New York, 1994, Vol. 6, p 2903.
(7) Haertling, G. H. *Ceramic Materials for Electronics*, 2nd ed.; Dekker: New York, 1991, p 129.
(8) Leverenz, H. W. *Luminescence of Solids*; Wiley: New York, 1980.
(9) Einzinger, R. *Annu. Rev. Mater. Sci*. **1987**, *17*, 299.
(10) Tarascon, J.-M.; Barboux, P.; Miceli, R. F.; Greene, L. H.; Hull, G. W.; Elbschutz, M.; Sunshine, S. A. *Phys. Rev*. **1988**, *B37*, 7458.
(11) Matkin, D. I. *Modern Oxide Materials*; Academic Press: New York, 1972, p 235.
(12) Rao, C. N. R.; Rao, K. I. *Solid State Compounds*; Clarendon Press: Oxford, 1992, p 281.
(13) Bierlein, J. D.; Arweiler, C. B. *Appl. Phys. Lett*. **1987**, *49*, 917.
(14) Centi, G.; Trifuro, F.; Ebner, J. R.; Franchetti, V. M. *Chem. Rev*. **1988**, *88*, 55.
(15) Grasselli, R. K. *Appl. Catal*. **1985**, *15*, 127.
(16) Gasior, M.; Gasior, I.; Grzybowska, B. *Appl. Catal*. **1984**, *10*, 87.
(17) Okuhara, T.; Misono, M. *Encyclopedia of Inorganic Chemistry*; John Wiley and Sons: New York, 1994; Vol. 6, p 2889.
(18) Niiyama, H.; Echigoya, E. *Bull. Chem. Soc. Jpn*. **1972**, *45*, 83.
(19) Yamaguchi, T. *Appl. Catal*. **1990**, *61*, 1.
(20) Clearfield, A. *Chem. Rev*. **1988**, *88*, 125.
(21) Newsam, J. M. *Solid State Compounds*; Clarendon Press: Oxford, 1992; p 234.
(22) Ruthven, D. M. *Principles of Absorption and Absorption Processes*; Wiley-Interscience: New York, 1984.
(23) Szostak, R. *Molecules Sieves. Principles of Synthesis and Identification*; Van Nostrand: Rheinhold, New York, 1988.
(24) Raleo, J. A. *Zeolite Chemistry and Catalysis*; ACS Monograph 7; American Chemical Society: Washington, DC, 1976.
(25) *New Developments in Zeolite Science*; Murakami, Y., Iijima, A., Ward, J. W., Eds.; Elsevier: Amsterdam, 1986.
(26) (a) Vaughan, D. E. W. *Properties and Applications of Zeolites*; Chem. Soc. Special Publication No. 33; The Chemical Society: London, 1979, p 294. (b) Cheetham, A. K. *Science* **1994**, *264*, 794.
(27) Venuto, P. B. *Microporous Mater*. **1994**, *2*, 297.
(28) Mallouk, T. E.; Lee, H. *J. Chem. Educ*. **1990**, *67*, 829.
(29) Stein, A.; Keller, S. W.; Mallouk, T. E. *Science* **1993**, *259*, 1558.

10.1021/ic011124v CCC: $22.00
Published on Web 03/21/2002

of novel compositions and architectures. For example, it is clear from the study of many naturally occurring, structurally complex mineral species that hydrothermal synthesis[30,31] provides a low temperature pathway to open framework, metastable structures from a variety of inorganic starting materials. It has also been abundantly demonstrated in the past decade that organic components can dramatically influence oxide microstructure.[32] The synergism between organic and inorganic components may be exploited in the preparation of hybrid materials exhibiting composite or even new properties. The organic component may be used to imprint structural information onto the inorganic scaffolding. Furthermore, the hydrothermal method is nicely suited to the preparation of such hybrid materials because it provides a means to overcome differential solubilities of inorganic oxides and organic precursors and to avoid phase separation. The general approach of employing organic materials at low temperature to modify or control the surface of growing oxide crystals in a hydrothermal medium has been exploited in the organic-directed crystallizations of oxide materials such as zeolites,[33−35] mesoporous oxides of the MCM-41 class,[36] and metal phosphates with entrained organic cations.[37−54]

While the organic components in these examples serve as charge-compensating cations and space-filling structural subunits, these species may also be introduced as ligands, tethered directly to the metal oxide substructure or to a secondary metal site. Thus, the structural influences of organonitrogen ligands in vanadium and molybdenum oxides are apparent in materials such as $[MoO_3(4,4'\text{-bipyridine})_{0.5}]$, $[MoO_3(\text{triazole})_{0.5}]$, and $[V_9O_{22}(\text{terpyridine})_3]$.[55,56] Principles of fundamental coordination chemistry may also be applied to the modification of oxide microstructure in hybrid materials. In this case, the organic component acts as a ligand to a secondary metal site, which is in turn directly coordinated through bridging oxo-groups to the oxide substructure. Consequently, the overall structure reflects both the geometric constraints of the ligand, as manifested in the size, shape, relative dispositions of the donor groups, and denticity, as well as the coordination preferences of the secondary metal site, as reflected in the coordination number and geometry, degree of aggregation into oligomeric units, and mode of attachment to the primary metal oxide scaffolding. This general strategy has been exploited by us in the development of the structural chemistries of two families of materials: the vanadium oxides of the type V/O/M′/ligand[57−63] and the molybdenum oxides of the Mo/O/M′/ligand family.[64−81]

(30) Rabenau, A. *Angew. Chem., Int. Ed. Engl.* **1985**, *24*, 1026.
(31) Gopalakrishnan, J. *Chem. Mater.* **1995**, *7*, 1265.
(32) (a) Stupp, S. I.; Braun, P. V. *Science* **1997**, *277*, 1242. (b) Davis, M. E.; Katz, A.; Ahmad, W. R. *Chem. Mater.* **1996**, *8*, 1820.
(33) (a) Newsam, J. M. Zeolites. In *Solid State Chemistry: Compounds*; Clarendon Press: Oxford, 1992; p 234. (b) Raleo, J. A. *Zeolite Chemistry and Catalysis*; ACS Monograph 7; American Chemical Society: Washington, DC, 1976. (c) *New Development in Zeolite Science*; Murakami, Y., Iijima, A., Ward, J. W., Eds.; Elsevier: Amsterdam, 1986. (d) Vaughan, D. E. W. *Properties and Applications of Zeolites*; Chemical Society Special Publication No. 33; The Chemical Society: London, 1979, p 294. (e) Venuto, P. B. *Microporous Mater.* **1994**, *2*, 297. (f) Szostak, R. *Molecular Sieves − Principles of Synthesis and Identification*, 2nd ed.; Van Nostrand Rheinhold, New York, 1997.
(34) (a) Smith, J. V. *Chem. Rev.* **1988**, *88*, 149. (b) Occelli, M. L.; Robson, H. C. *Zeolite Synthesis*; American Chemical Society: Washington, DC, 1989.
(35) Barrer, R. M. *Hydrothermal Chemistry of Zeolites*; Academic Press: New York, 1982.
(36) Kresge, C. T.; Leonowicz, M. E.; Roth, W. J.; Vartuli, J. C.; Beck, J. S. *Nature* **1992**, *359*, 710.
(37) The oxomolybdenum phosphates with entrained organic cations have been reviewed: Haushalter, R. C.; Mundi, L. A. *Chem. Mater.* **1992**, *4*, 31. Refs 39−54 are representative examples of the expansive family of oxovanadium/phosphate/organic cation materials.
(38) Khan, M. L.; Meyer, L. M.; Haushalter, R. C.; Schweitzer, C. L.; Zubieta, J.; Dye, J. L. *Chem. Mater.* **1996**, *8*, 43.
(39) Khan, M. I.; Haushalter, R. C.; O'Connor, C. J.; Tao, C.; Zubieta, J. *Chem. Mater.* **1995**, *7*, 593.
(40) Bircsak, Z.; Hall, A. K.; Harrison, W. T. A. *J. Solid State Chem.* **1999**, *142*, 168.
(41) Chippindale, A. M. *Chem. Mater.* **2000**, *12*, 818.
(42) (a) Soghomonian, V.; Haushalter, R. C.; Chen, Q.; Zubieta, J. *Inorg. Chem.* **1994**, *33*, 1700. (b) Riou, D.; Ferey, G. *Eur. J. Solid State Inorg. Chem.* **1994**, *31*, 25.
(43) Lu Y.; Haushalter, R. C.; Zubieta, J. *Inorg. Chim. Acta* **1997**, *257*, 268.
(44) Bircsak, Z.; Harrison, W. T. A. *Inorg. Chem.* **1998**, *37*, 3204.
(45) Finn, R. C.; Zubieta, J. Unpublished results.
(46) Soghomonian, V.; Chen, Q.; Zhang, Y.; Haushalter, R. C.; O'Connor, C. J.; Tao, C.; Zubieta, J. *Inorg. Chem.* **1995**, *34*, 3509.
(47) Soghomonian, V.; Chen, Q.; Haushalter, R. C.; Zubieta, J.; O'Connor, C. J.; Lee, Y.-S. *Chem. Mater.* **1993**, *5*, 1690.
(48) Loiseau, T.; Férey, G. *J. Solid State Chem.* **1994**, *111*, 416.
(49) Soghomonian, V.; Chen, Q.; Haushalter, R. C.; Zubieta, J. *Chem. Mater.* **1993**, *5*, 1595.
(50) Soghomonian, V.; Haushalter, R. C.; Zubieta, J.; O'Connor, C. J. *Inorg. Chem.* **1996**, *35*, 2826.
(51) Bu, X.; Feng, P.; Stucky, G. D. *Chem. Commun.* **1995**, 1337.
(52) Soghomonian, V.; Chen, Q.; Haushalter, R. C.; Zubieta, J. *Angew. Chem., Int. Ed. Engl.* **1993**, *32*, 610.
(53) Harrison, W. T. A.; Hsu, K.; Jacobson, A. J. *Chem. Mater.* **1995**, *7*, 2004.
(54) Zhang, Y.; Clearfield, A.; Haushalter, R. C. *Chem. Mater.* **1995**, *7*, 1221.
(55) Hagrman, P. J.; LaDuca, R. L., Jr.; Koo, H.-J.; Rarig, R. S., Jr.; Haushalter, R. C.; Whangbo, M.-H.; Zubieta, J. *Inorg. Chem.* **2000**, *39*, 4311.
(56) Hagrman, P. J.; Zubieta, J. *Inorg. Chem.* **2000**, *39*, 3252.
(57) Zhang, Y.; DeBord, J. R. D.; O'Connor, C. J.; Haushalter, R. C.; Clearfield, A.; Zubieta, J. *Angew. Chem., Int. Ed. Engl.* **1996**, *35*, 989.
(58) DeBord, J. R. D.; Zhang, Y.; Haushalter, R. C.; Zubieta, J.; O'Connor, C. J. *Solid State Chem.* **1996**, *122*, 251.
(59) LaDuca, R. L., Jr.; Finn, R. C.; Zubieta, J. *Chem. Commun.* **1999**, 1669.
(60) LaDuca, R. L., Jr.; Rarig, R. S., Jr.; Zubieta, J. *Inorg. Chem.* **2001**, *40*.
(61) Ollivier, P. J.; DeBord, J.R. D.; Zapf, P. J.; Zubieta, J.; Meyer, L. M.; Wang, C.-C.; Mallouk, T. E.; Haushalter, R. C. *THEOCHEM* **1998**, *470*, 49.
(62) Hagrman, P. J.; Bridges, C.; Greedan, J. E.; Zubieta, J. *J. Chem. Soc., Dalton Trans.* **1999**, 2901.
(63) LaDuca, R. C., Jr.; Brodkin, C.; Finn, R. C.; Zubieta, J. *Inorg. Chem. Commun.* **2000**, *3*, 248.
(64) Hagrman, P. J.; Hagrman, D.; Zubieta, J. *Angew. Chem., Int. Ed.* **1999**, *38*, 2638.
(65) Hagrman, D.; Zubieta, C.; Haushalter, R. C.; Zubieta, J. *Angew. Chem., Int. Ed. Engl.* **1997**, *36*, 873.
(66) Hagrman, D.; Sangregorio, C.; O'Connor, C. J.; Zubieta, J. *J. Chem. Soc., Dalton Trans.* **1998**, 3707.
(67) Hagrman, D.; Hagrman, P.; Zubieta, J. *Inorg. Chim. Acta* **2000**, *300−302*, 212.
(68) DeBord, J. R. D.; Haushalter, R. C.; Meyer, L. M.; Rose, D. J.; Zapf, P. J.; Zubieta, J. *Inorg. Chim. Acta* **1997**, *256*, 165.
(69) Hagrman, D.; Zapf, P. J.; Zubieta, J. *Chem. Commun.* **1998**, 1283.
(70) Hagrman, D.; Hagrman, P. J.; Zubieta, J. *Angew. Chem., Int. Ed* **1999**, *38*, 3165.
(71) Hagrman, D.; Zubieta, J. *C. R. Acad. Sci., Ser. IIc: Chim.* **2000**, *3*, 231.
(72) Hagrman, D.; Hagrman, P. J.; Zubieta, J. *Comments Inorg. Chem.* **1999**, *21*, 225 and references therein.
(73) Chesnut, D. J.; Hagrman, D.; Zapf, P. J.; Hammond, R. P.; LaDuca, R., Jr.; Haushalter, R. C.; Zubieta, J. *Coord. Chem. Rev.* **1999**, *190−192*, 737.
(74) Zapf, P. J.; Hammond, R. P.; Haushalter, R. C.; Zubieta, J. *Chem. Mater.* **1998**, *10*, 1366.

The molybdenum oxide hybrid materials in many cases are constructed from molecular cluster building blocks, derived from the vast family of polyoxomolybdate anions.[82] Consequently, these materials are related to general efforts to construct specific architectures from molecular building blocks, exemplified by coordination polymers[83] and cluster-based materials[84] from the expansive literature of "crystal engineering".[85,86] The use of well-defined molecular oxide clusters for the construction of solids with more or less predictable connectivity in the crystalline state is attractive, because secondary metal/ligand bridges should provide linkages sufficiently strong to connect the clusters into kinetically stable, crystalline architectures. In this respect, the polyoxomolybdate−organophosphonates[87] of the type $[Mo_5O_{15}(O_3PR)_2]^{4-}$ should provide building blocks for the construction of one-dimensional organic/inorganic oxides through tethering of the organophosphonate components with appropriate organic linkers. We recently demonstrated that this naive expectation could be realized but only in the presence of a secondary metal/organic subunit, as in $[\{Cu(H_2O)_2(o\text{-phen})\}\{Cu(o\text{-phen})_2\}(Mo_5O_{15})(O_3PCH_2CH_2CH_2PO_3)]\cdot 2.5H_2O$.[88] In fact, the preparation of this latter one-dimensional material represents a confluence of the themes of hydrothermal synthesis, organic/inorganic hybrid materials, structural modification by secondary metal/ligand subunits, and tethering of molecular cluster building blocks. As part of our systematic studies of the copper−molybdenum oxide/organophosphonate/organoimine materials, we have synthesized and structurally characterized a series of one- and two-dimensional materials, by varying the tether length of the diphosphonate ligands, $\{O_3P(CH_2)_nPO_3\}^{4-}$ ($n = 1$, 2, 3 and 4), and the identity of the organoimine ligand, 2,2′-bipyridine and terpyridine. The structural influences of the tether lengths and reaction conditions are manifested in the structures of $[Cu(bpy)(MoO_2)(H_2O)(O_3PCH_2PO_3)]$ (**1**), $[Cu(bpy)(Mo_2O_5)(H_2O)(O_3PCH_2PO_3)]\cdot H_2O$ (**2**·H_2O), $[\{Cu(bpy)\}_2(Mo_4O_{12})(H_2O)_2(O_3PCH_2CH_2PO_3)]\cdot 2H_2O$ (**3**·$2H_2O$), $[Cu(bpy)(Mo_2O_5)(O_3PCH_2CH_2CH_2PO_3)]$ (**4**), $[\{Cu(bpy)_2\}\{Cu(bpy)(H_2O)\}(MO_5O_{15})(O_3PCH_2CH_2CH_2CH_2PO_3)]\cdot H_2O$ (**5**·H_2O), $[Cu(terpy)(Mo_2O_5)(O_3PCH_2PO_3)]$ (**6**), $[\{Cu(terpy)(H_2O)\}_2(Mo_5O_{15})(O_3PCH_2CH_2PO_3)]\cdot 3H_2O$ (**7**·$3H_2O$), and $[\{Cu(terpy)\}_2(Mo_5O_{15})\ (O_3PCH_2CH_2CH_2PO_3)]$ (**8**).

Experimental Section

Compounds were prepared using 23 mL Parr acid digestion bombs with Teflon liners as reaction vessels. Syntheses were carried out under autogenous pressure with fill volumes of ∼35%. All reagents were used as received from Aldrich Chemical Co. Water was distilled above 3.0 Ω in-housing using a Barnstead model 525 Biopure distilled water center.

Synthesis of $[Cu(bpy)(MoO_2)(H_2O)(O_3PCH_2PO_3)]$ (1). A solution of $Cu(CH_3CO_2)_2\cdot H_2O$ (0.049 g, 0.249 mmol), MoO_3 (0.05 g, 0.391 mmol), 2,2′-bipyridine (0.047 g, 0.301 mmol), methylene diphosphonic acid (0.056 g, 0.318 mmol), water (11.53 g, 640 mmol), and acetic acid (0.110 g, 1.83 mmol) was stirred briefly and heated to 150° C for 120 h. Light blue plates of **1** were recovered in 70% yield, with dark blue plates of **2** accounting for the remaining material. Crystals of **1** were separated mechanically for subsequent study. IR (KBr pellet, cm^{-1}): 1638 (m), 1602 (m), 1560 (s), 1444 (s), 1144 (m), 1027 (m), 891 (m), 782 (m), 670 (s). Anal. Calcd for $C_{11}H_{12}CuMoN_2O_9P_2$: C, 24.6; H, 2.25; N, 5.21. Found: C, 24.3; H, 2.17; N, 5.33.

Synthesis of $[Cu(bpy)(Mo_2O_5)(H_2O)(O_3PCH_2PO_6)]\cdot H_2O$ (2·H_2O). When the reaction that produced compound **1** is carried out for a shorter time period, 60 h at 150° C, dark blue blocks of **2** are isolated in 60% yield. IR (KBr pellet, cm^{-1}): 1604 (m), 1448 (s), 1157 (s), 1111 (m), 1008 (m), 947 (m), 921 (s), 879 (s), 679 (m). Anal. Calcd for $C_{11}H_{14}CuMo_2N_2O_{13}P_2$: C, 18.9; H, 2.02; N, 4.00. Found: C, 18.8; H, 2.11; N, 3.88.

Synthesis of $[\{Cu(bpy)\}_2(Mo_4O_{12})(H_2O)_2(O_3PCH_2CH_2PO_3)]\cdot 2H_2O$ (3·$2H_2O$). A solution of $CuSO_4\cdot 5H_2O$ (0.036 g, 0.144 mmol), 2,2′-bipyridine (0.044 g, 0.282 mmol), $Na_2MoO_4\cdot 2H_2O$ (0.084 g, 0.347 mmol), 1,2-ethylene diphosphonic acid, and water (10.24 g, 568 mmol) in the mole ratio 1.00:1.96:2.41:1.79:3944 was heated to 180° C for 39 h. Upon cooling, blue needles of **3** were collected in 35% yield. IR (KBr pellet, cm^{-1}): 1602 (s), 1445 (s), 1192 (s),

(75) Hagrman, D.; Warren, C. J.; Haushalter, R. C.; Seip, C.; O'Connor, C. J.; Rarig, R. S., Jr.; Johnson, K. M., III.; LaDuca, R. L., Jr.; Zubieta, J. *Chem. Mater.* **1998**, *10*, 3294.
(76) Hagrman, D.; Haushalter, R. C.; Zubieta, J. *Chem. Mater.* **1998**, *10*, 361.
(77) Laskoski, M. C.; LaDuca, R. L., Jr.; Rarig, R. S., Jr.; Zubieta, J. *Chem. Soc., Dalton Trans.* **1999**, 3467.
(78) Hagrman, D. E.; Zubieta, J. *J. Solid State Chem.* **2000**, *152*, 141.
(79) LaDuca, R. L., Jr.; Desciak, M.; Laskoski, M.; Rarig, R. S., Jr.; Zubieta, J. *J. Chem. Soc., Dalton Trans.* **2000**, 2255.
(80) Zapf, P. J.; Warren, C. J.; Haushalter, R. C.; Zubieta, J. *Chem. Commun.* **1997**, 1543.
(81) Aschwanden, S.; Schmalle, H. W.; Reller, A.; Oswald, H. R. *Mater. Res. Bull.* **1993**, *28*, 45. For other examples of the V/O/M′/ligand family see also: (a) Lin, B.-Z.; Liu, S.-X. *Polyhedron* **2000**, *19*, 2521. (b) Zheng, L.-M.; Zhao, J.-S.; Lii, K.-H.; Zhang, L.-Y.; Liu, Y.; Xin, X.-Q. *J. Chem. Soc., Dalton Trans.* **1999**, 939. (c) Chen, R.; Zavalij, P. Y.; Whittingham, M. S.; Greedan, J. E.; Raju, N. P.; Bieringer, M. *J. Mater. Chem.* **1999**, 93. (d) Shi, Z.; Zhang, L.; Zhu, G.; Yang, G.; Hua, J.; Ding, H.; Feng, S. *Chem. Mater.* **1999**, *11*, 3565. (e) Law, T. S.-C.; Williams, I. D. *Chem. Mater.* **2000**, *12*, 2070. (f) Zheng, L.-M.; Whitfield, T.; Wang, X.; Jacobson, A. J. *Angew. Chem., Int. Ed.* **2000**, *39*, 4528.
(82) Pope, M. T. *Heteropoly and Isopoly Oxometalates*; Springer: New York, 1983.
(83) See, for example: (a) Hoskins, B. F.; Robson, R. *J. Am. Chem. Soc.* **1990**, *112*, 1546. (b) Yaghi, O. M.; Li, H. *J. Am. Chem. Soc.* **1995**, *117*, 10401. (c) Carlucci, L.; Gianfranco, C.; Prosperio, D. M.; Sironi, A. *J. Am. Chem. Soc.* **1995**, *117*, 12861. (d) MacGillivray, L. R.; Subramanian, L. R.; Zaworotko, M. J. *J. Chem. Soc., Chem. Commun.* **1994**, 1325. (e) Blake, A. J.; Champness, N. R.; Chung, S. S. M.; Li, W.-S.; Schröder, M. *Chem. Commun.* **1997**, 1005. (f) Noro, S.; Kitagawa, S.; Kondo, M.; Seki, K. *Angew. Chem., Int. Ed.* **2000**, *39*, 2082. (g) Carlucci, L.; Ciani, G.; Prosperio, D. M.; Rizzata, S. *Chem. Commun.* **2000**, 1319. (h) Reineke, T. M.; Eddaoudi, M.; Moler, D.; O'Keefe, M.; Yaghi, O. M. *J. Am. Chem. Soc.* **2000**, *122*, 4843.
(84) See, for example: (a) Naumov, N. G.; Virovets, A. V.; Sokolov, M. N.; Artemkina, S. B.; Fedorov, V. E. *Angew. Chem., Int. Ed.* **1998**, *37*, 1943. (b) Beauvais, L. G.; Shores, M. P.; Long, J. R. *Chem. Mater.* **1998**, *10*, 3783. (c) Shores, M. P.; Beauvais, L. G.; Long, J. R. *J. Am. Chem. Soc.* **1999**, *121*, 775. (d) Müller, A.; Das, S. K.; Kögerler, P.; Bögge, H.; Schmidtmann, M.; Trautwein, A. X.; Schünemann, V.; Krickmeyer, E.; Preetz, W. *Angew. Chem., Int. Ed.* **2000**, *39*, 3414. (e) Khan, M. I.; Yohannes, E.; Powell, D. *Inorg. Chem.* **1999**, *38*, 212. (f) Ouahab, L. *C. R. Acad. Sci., Ser. IIc: Chim.* **1998**, 369. (g) Galán-Mascarós, J.; Giménez-Saiz, C.; Triki, S.; Gómez-Garcia, C. J.; Coronado, E.; Quahab, L. *Angew. Chem., Int. Ed.* **1995**, *34*, 1460. (h) Sadakane, M.; Dickman, M. H.; Pope, M. T. *Angew. Chem., Int. Ed.* **2000**, *39*, 2914. (i) Krebs, B.; Loose, I.; Bösing, M.; Nöh, A.; Droste, E. *C. R. Acad. Sci., Ser. IIc: Chim.* **1998**, 351. (j) Stein, A.; Fendorf, M.; Jarvie, T. P.; Mueller, K. T.; Bensei, A. J.; Mallouk, T. E. *Chem. Mater.* **1995**, *7*, 304. (k) Holland, B. T.; Isbester, P. K.; Munson, E. J.; Stein, A. *Mater. Res. Bull.* **1999**, *34*, 471.
(85) Ferey, G. *J. Solid State Chem.* **2000**, *152*, 37.
(86) Zaworotko, M. J. *Angew. Chem., Int. Ed.* **2000**, *39*, 3052.
(87) Kwak, W.; Pope, M. T.; Scully, T. F. *J. Am. Chem. Soc.* **1975**, *97*, 5735.
(88) Finn, R. C.; Zubieta, J. *Inorg. Chem.* **2001**, *40*, 2466.

1161 (m), 1048 (m), 1004 (s), 940 (s), 913 (m), 769 (s), 730 (m), 670 (m). Anal. Calcd for $C_{11}H_{14}N_2O_{11}Mo_2CuP$: C, 20.8; H, 2.22; N, 4.40. Found: C, 20.6; H, 2.10; N, 4.22.

Synthesis of [Cu(bpy)(Mo_2O_5)($O_3PCH_2CH_2CH_2PO_3$)] (4). A solution of $CuSO_4 \cdot 5H_2O$ (0.087 g, 0.348 mmol), 2,2′-bipyridine (0.050 g, 0.320 mmol), MoO_3 (0.056 g, 0.438 mmol), 1,3′-propylene diphosphonic acid (0.083 g, 0.407 mmol), and water (10.57, 586 mmol) in the mole ratio 1.09:1.00:1.37:1.27:1831 was heated to 180° C for 42.5 h. The reaction was allowed to cool slowly in the oven at a rate of about 20° C/h until reaching room temperature, whereupon blue crystals of **4** were isolated in 30% yield. IR (KBr pellet, cm^{-1}): 1602 (m), 1443 (s), 1160 (m), 1107 (m), 1059 (m), 939 (m), 906 (m), 772 (s), 698 (m), 620 (s). Anal. Calcd for $C_{13}H_{14}CuMo_2N_2O_{11}P_2$: C, 22.6; H, 2.04; N, 4.05. Found: C, 22.9; H, 2.11; N, 3.99.

Synthesis of [{Cu(bpy)$_2$}{Cu(bpy)(H_2O)}(Mo_5O_{15})($O_3PCH_2CH_2CH_2CH_2PO_3$)]·H_2O (5·H_2O). A solution of $CuSO_4 \cdot 5H_2O$ (0.037 g, 0.14 mmol), $Na_2MoO_4 \cdot 2H_2O$ (0.062 g, 0.256 mmol), 2,2′-bipyridine (0.062 g, 0.284 mmol), and water (10.20 g, 566 mmol) in the mole ratio 1.00:1.73:1.92:2.51:3756 was stirred briefly before heating to 180° C for 39 h. Blue crystals of **5** were recovered in 30% yield. IR (KBr pellet, cm^{-1}): 1654 (s), 1559 (s), 1473 (m), 1447 (s), 1124 (br), 1061 (br), 1034 (s), 984 (m), 916 (s), 767 (s), 699 (br). Anal. Calcd for $C_{34}H_{36}Cu_2Mo_5N_6O_{23}P_2$: C, 26.4; H, 2.35; N, 5.43. Found: C, 26.3; H, 2.20; N, 5.22.

Synthesis of [Cu(terpy)(Mo_2O_5)($O_3PCH_2PO_3$)] (6). A solution of $CuSO_4 \cdot 5H_2O$ (0.036 g, 0.144 mmol), terpyridine (0.062 g, 0.244 mmol), MoO_3 (0.062 g, 0.485 mmol), methylene diphosphonic acid (0.076 g, 0.432 mmol), and water (10.40 g, 577 mmol) in the mole ratio 1.00:1.69:3.37:3.00:4000 was heated to 180° C for 39 h. Blue plates of **6** were collected in 40% yield. IR (KBr pellet, cm^{-1}): 1601 (m), 1444 (s), 1170 (m), 1144 (m), 1027 (m), 925 (s), 912 (m), 782 (s), 732 (s), 669 (br). Anal. Calcd for $C_{16}H_{13}CuMo_2N_3O_{11}P_2$: Anal. Calcd for $C_{16}H_{13}CuMo_2N_3O_{11}P_2$: C, 25.9; H, 1.77; N, 5.67. Found: C, 30.2; H, 1.71; N, 5.62.

Synthesis of [{Cu(terpy)(H_2O)}$_2$(Mo_5O_{15})($O_3PCH_2CH_2PO_3$)]·3H_2O(7·3H_2O). A solution of $Cu(CH_3CO_2)_2 \cdot H_2O$ (0.130 g, 0.651 mmol), terpyridine (0.080 g, 0.343 mmol), MoO_3 (0.139 g, 0.966 mmol), 1,2-ethylene diphosphonic acid (0.086 g, 0.453 mmol), and water (10.34 g, 574 mmol) in the mole ratio 1.90:1.00:2.82:1.32:1673, with sufficient acetic acid to lower the pH to ~3−4, was heated to 180° C for 44.5 h. Dark blue needles of **7** were isolated in 40% yield. IR (KBr pellet, cm^{-1}): 1647 (m), 1559 (s), 1540 (m), 1474 (m), 1193 (s), 1163 (m), 1124 (br), 998 (m), 894 (br), 775 (br),689 (m). Anal. Calcd for $C_{32}H_{36}Cu_2Mo_5N_6O_{26}P_2$: C, 24.2; H, 2.28; N, 5.29. Found: C, 23.8; H, 2.11; N, 5.44.

Synthesis of [{Cu(terpy)}$_2$(Mo_5O_{15})($O_3PCH_2CH_2CH_2PO_3$)] (8). A solution of $Cu(CH_3CO_2)_2 \cdot H_2O$ (0.120 g, 0.601 mmol), terpyridine (0.072 g, 0.309 mmol), MoO_3 (0.267 g, 1.85 mmol), 1,3′-propylene diphosphonic acid (0.177 g, 0.868 mmol), and water (10.74 g, 596 mmol) in the mole ratio 1.94:1:00:6.00:2.81:1929, with enough acetic acid to lower the pH to ~3−4, was heated to 180° C for 44.5 h. Blue blocks of **8** were collected in 45% yield. IR (KBr pellet, cm^{-1}): 1602 (m), 1477 (m), 1451 (m), 1106 (s), 1020 (m), 966 (s), 921 (m), 880 (s), 749 (m), 676 (m), 631 (m). Anal. Calcd for $C_{33}H_{28}Cu_2Mo_5N_6O_{21}P_2$: C, 26.2; H, 1.92; N, 5.55. Found: C, 26.3; H, 1.77; N, 5.31.

X-ray Crystallography. Structural measurements for **1**−**8** were performed on a Bruker SMART-CCD diffractometer using graphite monochromated Mo Kα radiation (λ(Mo Kα) = 0.71073 Å). Data were collected at 90(2) K. Data were corrected for Lorentz and polarization effects. Data reduction was performed using SAINT, and an empirical absorption correction was made using SADABS.[89] The structures of **1**−**8** were solved via direct methods.[90] All non-hydrogen atoms in **1**−**8** were refined anisotropically. Neutral atom scattering coefficients and anomalous dispersion corrections were taken from International Tables Vol. C.[91] Calculations were performed using the SHELXTL crystallographic software package.[90] The model was refined against F^2 until the final value of Δ/T_{max} was less than 0.001. The crystal data for **1**−**8** are summarized in Table 1. Because the metrical parameters associated with these structures are unexceptional, bond lengths and angles are given in the tables found in Supporting Information only.

Results and Discussion

The preparation of compounds **1**−**8** relies on hydrothermal methods, which have now been demonstrated as effective in the synthesis of organic−inorganic hybrid materials of the molybdenum oxides,[92] vanadium oxides,[93] metal halides and pseudohalides,[94−97] as well as metal phosphates and organophosphonates. The method exploits the reduced viscosity of water at temperatures above 100° C and autogenous pressures to promote solvent extraction of solids and crystal growth from solution.

The syntheses proceeded in a relatively straightforward fashion from a Cu(II) source, a Mo(VI) source, an organoimine ligand, and the appropriate organodiphosphonate ligand. Optimization of yields and monophasic products required manipulations of stoichiometries, reaction pH, and identities of the transition metal starting materials. Consequently, $CuSO_4 \cdot 5H_2O$ was found more effective in certain cases than $Cu(CH_3CO_2)_2 \cdot H_2O$. Similarly, $Na_2MoO_4 \cdot 2H_2O$ was used in place of MoO_3 in a number of reactions. Optimal conditions for the preparations of **1**, **2**, **7**, and **8** required addition of acetic acid to lower the pH to ~3−4 from the value of 6−6.5 used in the syntheses of **3**−**6**. Lowering the pH below 2.5 or raising it above 7.0 resulted in intractable mixtures of amorphous materials in all cases. It is also noteworthy that small changes in reaction conditions often result in different products. Thus, the reaction of [$Cu(CH_3CO_2)_2$]·H_2O, MoO_3, 2,2′-bipyridine, methylenediphosphonate, and acetic acid in water in a mole ratio 1:1.57:1.21:1.28:7.35:2570 at 150° C for 120 h yielded light blue plates of **1**; however, if the reaction time is decreased to 60 h, dark blue plates of **2**·H_2O are recovered as the major product.

The infrared spectra of **1**−**8** exhibit three peaks in the 960−1160 cm^{-1} range attributed to ν(P—O) bands of the

(89) *SAINT+*, Version 6.02; Brüker AXS: Madison, WI, 1999.
(90) *SHELXTL*, Version 5.1; Brüker AXS: Madison, WI, 1998.
(91) *International Tables for Crystallography*; Kluwer Academic Publishers: Dordrecht, 1989; Vol. C, Tables 4.2.6.8 and 6.1.1.4.
(92) Hagrman, D.; Zubieta, J. *Trans. Am. Crystallogr. Assoc.* **1998**, *33*, 109.
(93) Hagrman, P. J.; Zubieta, J. *Inorg. Chem.* **2001**, *40*, 2800.
(94) Francis, R. J.; Halasyamani, P. S.; O'Hare, D. *Angew. Chem., Int. Ed.* **1998**, *37*, 2214.
(95) Mitzi, D. *Chem. Mater.* **1996**, *8*, 791.
(96) DeBord, J. R. D.; Lu, Y.-J.; Warren, C. J.; Haushalter, R. C.; Zubieta, J. *Chem. Commun.* **1997**, 1365.
(97) (a) Chesnut, D. J.; Kusnetzow, A.; Zubieta, J. *J. Chem. Soc., Dalton Trans.* **1998**, 4081. (b) Chesnut, D. J.; Zubieta, J. *Chem. Commun.* **1998**, 1707. (c) Chesnut, D. J.; Kusnetzow, A.; Birge, R. R.; Zubieta, J. *Inorg. Chem.* **1999**, *38*, 2663. (d) Chesnut, D. J.; Kusnetzow, A.; Birge, R. R.; Zubieta, J. *Inorg. Chem.* **1999**, *38*, 5484.

Table 1. Summary of Crystallographic Data for the Structure of [Cu(bpy)(MoO_2)(H_2O)($O_3PCH_2PO_3$)] (**1**), [Cu(bpy)(Mo_2O_5)(H_2O)($O_3PCH_2PO_3$)]·H_2O (**2**·H_2O), [{Cu(bpy)}$_2$(Mo_4O_{12})(H_2O)$_2$($O_3PCH_2CH_2PO_3$)]·2H_2O (**3**·2H_2O), [Cu(bpy)(Mo_2O_5)($O_3PCH_2CH_2CH_2PO_3$)] (**4**), [{Cu(bpy)$_2$}{Cu(bpy)(H_2O)(Mo_5O_{15})($O_3PCH_2CH_2CH_2CH_2PO_3$)]·H_2O (**5**·H_2O), [{Cu(terpy)(Mo_2O_5)($O_3PCH_2PO_3$)] (**6**), [{Cu(terpy)(H_2O)}$_2$(Mo_5O_{15})($O_3PCH_2CH_2PO_3$)]·3H_2O (**7**·3H_2O), and [{Cu(terpy)}$_2$(Mo_5O_{15})($O_3PCH_2CH_2CH_2PO_3$)] (**8**)

	1	**2**	**3**	**4**
empirical formula	$C_{11}H_{12}CuMoN_2O_9P_2$	$C_{11}H_{14}CuMo_2N_2O_{13}P_2$	$C_{11}H_{14}CuMo_2N_2O_{11}P$	$C_{13}H_{14}CuMo_2N_2O_{11}P_2$
fw	537.65	699.60	636.63	691.62
space group	$P\bar{1}$	*Pbca*	$P\bar{1}$	$P2_1/c$
a, Å	8.0801(4)	7.828(1)	8.0759(3)	8.5535(8)
b, Å	8.6606(5)	19.877(3)	10.2293(4)	24.723(2)
c, Å	11.8803(6)	25.460(4)	12.4370(5)	9.6296(9)
α, deg	82.168(1)	90	70.758(1)	90
β, deg	77.847(1)	90	71.576(1)	105.726(2)
γ, deg	75.855(1)	90	71.508(1)	90
V, Å^3	784.93(7)	3962(1)	893.91(6)	1960.1(3)
Z	2	8	2	4
D_{calcd}, g cm^{-3}	2.275	2.346	2.365	2.344
μ, mm^{-1}	2.412	2.544	2.712	2.562
T, K	90(2)	90(2)	90(2)	90(2)
λ, Å	0.71073	0.71073	0.71073	0.71073
R1[a]	0.0344	0.0686	0.0312	0.0532
wR2[b]	0.0832	0.1396	0.0824	0.1207

	5	**6**	**7**	**8**
empirical formula	$C_{34}H_{36}Cu_2Mo_5N_6O_{23}P_2$	$C_{16}H_{13}CuMo_2N_3O_{11}P_2$	$C_{32}H_{36}Cu_2Mo_5N_6O_{22}P_2$	$C_{33}H_{28}Cu_2Mo_5N_6O_{21}P_2$
fw	1547.26	740.65	1589.39	1513.33
space group	$P\bar{1}$	$P2_1/n$	*C*2/*c*	*C*2/*c*
a, Å	11.3132(6)	8.5995(5)	16.494(1)	8.7047(6)
b, Å	12.8735(7)	20.853(1)	21.500(2)	23.371(2)
c, Å	18.297(1)	12.5137(7)	14.843(1)	19.719(2)
α, deg	71.690(1)	90	90	90
β, deg	82.910(1)	110.026(1)	121.128(1)	101.409(1)
γ, deg	65.580(1)	90	90	90
V, Å^3	2303.5(2)	2108.4(2)	4506.0(6)	3932.3(5)
Z	2	4	4	4
D_{calcd}, g cm^{-3}	2.231	2.333	2.343	2.556
μ, mm^{-1}	2.383	2.392	2.444	2.785
T, K	90.(2)	90.(2)	90.(2)	90.(2)
λ, Å	0.71073	0.71073	0.71073	0.71073
R1[a]	0.0545	0.0436	0.0698	0.0507
wR2[b]	0.1060	0.0812	0.1473	0.0891

[a] $R1 = \sum||F_o| - |F_c||/\sum|F_o|$ [b] $wR2 = \{\sum(w(F_o^2 - F_c^2)^2/\sum(w(F_o^2)^2)\}^{1/2}$

organodiphosphonate ligands. Prominent bands in the 1400−1640 cm^{-1} region are assigned to the bipyridine or terpyridine ligands. The location of the band associated with *ν*(Mo═O) exhibits considerable variability, 880−940 cm^{-1}, consistent with the range of structural types observed for **1**−**8**.

As shown in Figure 1a, the structure of [Cu(bpy)(MoO_2)(H_2O)($O_3PCH_2PO_3$)] (**1**) consists of one-dimensional chains, constructed from {MoO_6} octahedra, {CuN_2O_3} square pyramids, and {PCO_3} tetrahedra. The coordination sphere of the molybdenum is defined by three phosphonate oxygen donors, a terminal oxo-group, an oxo-group bridging to the copper, and an aqua ligand. Each Mo(VI) site is linked to three methylenediphosphonate ligands. The Cu(II) site adopts "4 + 1" square pyramidal geometry, with the basal plane occupied by two oxygen atoms from methylenediphosphonate ligands and two nitrogen donors from the bipyridine groups while the axial position is defined by a bridging oxo-group. Each methylenediphosphonate ligand chelates to a Cu(II) site through oxygen atoms on each phosphorus terminus to form a six-membered {Cu−O−P−C−P−O} ring and corner-shares with three {MoO_6} octahedra. Consequently, one oxygen is pendant.

The connectivity pattern results in a number of ring motifs, the most prominent of which is a twelve-membered {Mo−O−P−C−P−O−}$_2$ heterocycle. There are also eight-membered {Mo−O−P−O−}$_2$ and six-membered {Cu−O−Mo−O−P−O} and {Cu−O−P−C−P−O−} rings.

The overall structure of **1** may be described as {(MoO_2)(H_2O)($O_3PCH_2PO_3$)}$_n^{2n-}$ ribbons decorated with {Cu(bpy)}$^{2+}$ subunits. The aqua ligands project above and below the twelve-membered ring of the ribbon while the bpy ligands are directed into the intrachain regions where they interdigitate with bpy groups from neighboring chains, as illustrated in Figure 1b. The structure of **1** is quite distinct from that of the previously reported phenanthroline derivative [Cu(phen)(Mo_2O_5)($O_3PCH_2PO_3$)], shown in Figure 1c.[88] This latter structure not only exhibits a binuclear molybdate building block but also involves diphosphonate chelation to the molybdenum site rather than to the copper site.

In contrast to the one-dimensional structure of **1**, the structure of **2**·H_2O is two-dimensional, as shown in Figure 2. The network is constructed from binuclear units of edge-sharing {MoO_6} octahedra, Cu(II) square pyramids, and phosphorus tetrahedra. The two molybdenum environments of the binuclear subunit are quite distinct. The Mo(2) site is defined by two oxygen donors from the methylenediphosphonate ligands, a bridging oxo-group to the Mo(1) site, two *cis*-oriented terminal oxo-groups, and an aqua ligand. The

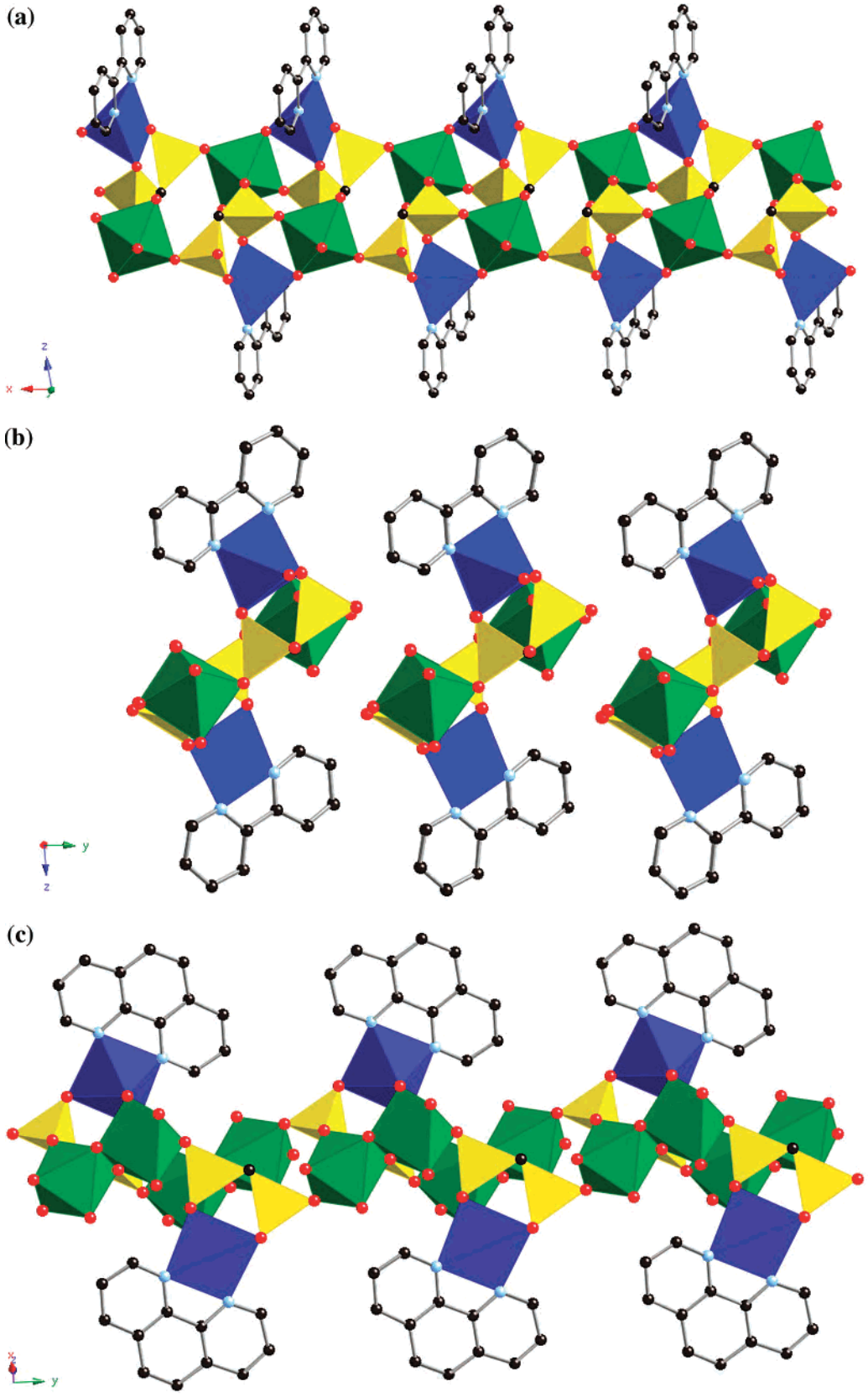

Figure 1. (a) View of the one-dimensional structure of [Cu(bpy)(MoO_2)(H_2O)($O_3PCH_2PO_3$)] (**1**), parallel to the crystallographic [011] direction. (b) View of the spatial relationship of neighboring chains of **1**. (c) Polyhedral representation of the structure of [Cu(phen)(Mo_2O_5)($O_3PCH_2PO_3$)].

Mo(1) site exhibits three oxygen donors from methylenediphosphonate ligands, a bridging oxo-group to Mo(2), a bridging oxo-group to the Cu(II) site, and a terminal oxo-group. The Mo(2) site shares two vertices with two methylenediphosphonate ligands and does not link to the Cu(II) center. The Mo(1) site shares three vertices with two

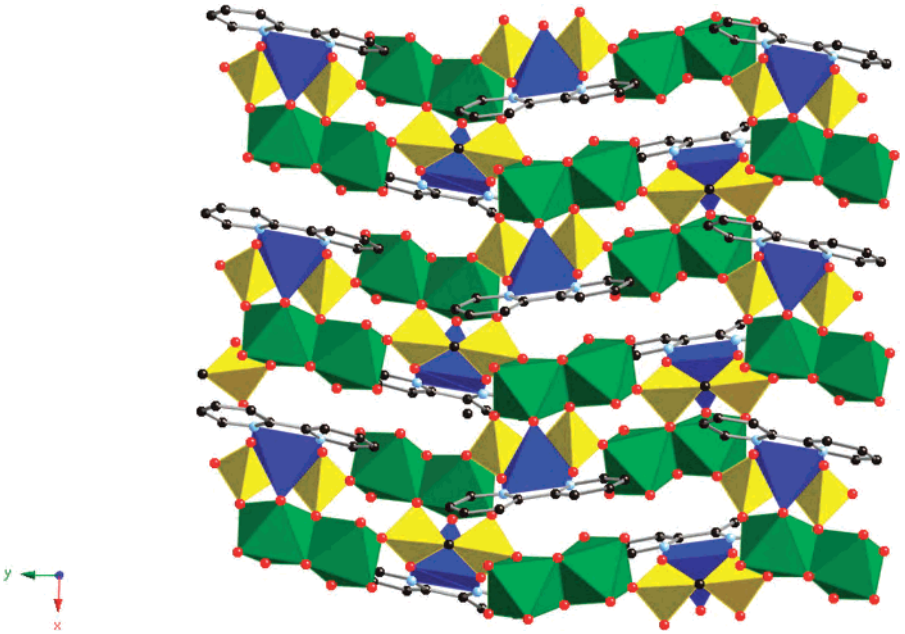

Figure 2. View of the two-dimensional structure of $[Cu(bpy)(Mo_2O_5)(H_2O)(O_3PCH_2PO_3)]\cdot H_2O$ (**2**·H_2O), parallel to the crystallographic *c* axis.

methylenediphosphonate ligands and one vertex with the copper. The Cu(II) site exhibits the common "4 + 1" square pyramidal geometry with the basal plane defined by two oxygen atoms of a chelating methylenediphosphonate ligand and the nitrogen donors of the bpy ligand and the apical position occupied by the oxo-group bridging to Mo(1).

Each methylenediphosphonate chelates not only to the Cu(II) site but also to the Mo(1) center to produce a $\{MoCu(O_3PCH_2PO_3)\}$ subunit. The remaining two oxygen atoms link the diphosphonate to two Mo(2) sites. Consequently, each diphosphonate ligand bonds to three binuclear Mo sites. In contrast to the structure of **1**, all of the oxygen atoms of the methylenediphosphonate ligand of **2** are involved in bonding.

The molybdophosphonate $\{(Mo_2O_5)(H_2O)(O_3PCH_2PO_3)\}_n^{2n-}$ substructure of **2** is two-dimensional, in contrast to the $\{(MoO_2)(H_2O)(O_3PCH_2PO_3)\}_n^{2n-}$ ribbon of **1**. The polyhedral connectivity generates 24-membered rings of six $\{MoO_6\}$ octahedra and six $\{O_3PR\}$ tetrahedra. The water molecules of crystallization occupy the internal cavities of these rings. There are also eight-membered $\{Mo-O-P-O-\}$ and six-membered $\{Mo-O-P-C-P-O-\}$ rings in the molybdophosphonate network. The $\{Cu(bpy)\}^{2+}$ moieties occupy positions associated with the $\{Mo-O-P-C-P-O-\}$ rings above and below the molybdophosphonate network.

An obvious feature of the structures of methylenediphosphonate derivatives **1** and **2** is the absence of phosphomolybdate cluster building blocks. This is a consequence of the limited spatial extension between $\{PO_3\}$ termini of the diphosphonate ligand provided by a single methylene tether. Consequently, rather than spanning component building blocks, the methylenediphosphonate ligand is geometrically suited to forming six-membered chelate rings to a single metal site, $\{M-O-P-C-P-O-\}$. This coordination preference is quite apparent in the previously reported oxovanadium phosphonate structures $Cs[(VO)(O_3PCH_2PO_3)]$,[98] $[H_2N(CH_2)_4NH_2]$ $[(VO)(O_3PCH_2PO_3)]$,[99] $Cs[(VO)_2V(O_3PCH_2PO_3)_2(H_2O)_2]$,[98] $[(VO)_2(O_3PCH_2PO_3)(H_2O)_4]$,[100] and $(NH_4)_2[(VO)(O_3PCH_2PO_3)]$.[101] The consequences of tether expansion are dramatically illustrated in the series of oxovanadate materials: the one-dimensional $[H_2N(CH_2)_4NH_2][(VO)(O_3PCH_2PO_3)]$, the two-dimensional $[H_3N(CH_2)_2NH_3][(VO)(O_3PCH_2CH_2PO_3)]$, and the three-dimensional $[H_3N(CH_2)_2NH_3]$ $[(VO)_4(OH)_2(H_2O)_2(O_3PCH_2CH_2CH_2PO_3)_2]$.[99] The dimensional expansion reflects the tether length of the diphosphonate ligands, which in the ethylene- and propylenediphosphonate materials link spatially distinct building blocks rather than chelating to a single vanadate polyhedron. The naive expectation was that the oxomolybdate/diphosphonate/Cu(II)/organoimine system would exhibit a similar trend and that under appropriate reaction conditions phosphomolybdate building blocks would be incorporated into the overall architectures. As we will see, the structural chemistry is not totally predictable and is influenced not only by tether lengths of the diphosphonate ligands but also by the identity of the organoimine coligand, as well as hydrothermal reaction conditions.

As shown in Figure 3a, the structure of $[\{Cu(bpy)\}_2(Mo_4O_{12})(H_2O)_2(O_3PCH_2CH_2PO_3)]\cdot 2H_2O$ (**3**·$2H_2O$) is a two-dimensional network constructed from tetranuclear oxomolybdate clusters linked through corner-sharing copper octahedra and diphosphonate ligands. The tetranuclear clusters consist of an "S" shaped array of edge-sharing Mo(VI) octahedra and square pyramids. An interior pair of base edge-sharing

(98) Bonavia, G.; Haushalter, R. C.; O'Connor, C. J.; Zubieta, J. *Inorg. Chem.* **1996**, *35*, 5603.
(99) Soghomonian, V.; Chen, Q.; Haushalter, R. C.; Zubieta, J. *Angew. Chem., Int. Ed. Engl.* **1995**, *34*, 223.
(100) Huan, G.; Johnson, J. W.; Jacobson, A. J.; Merola, J. S. *J. Solid State Chem.* **1990**, *89*, 220.
(101) Hinclaus, C.; Serre, C.; Riou, D.; Ferey, G. *C. R. Acad. Sci., Ser. IIc: Chim.* **1998**, *1*, 551.

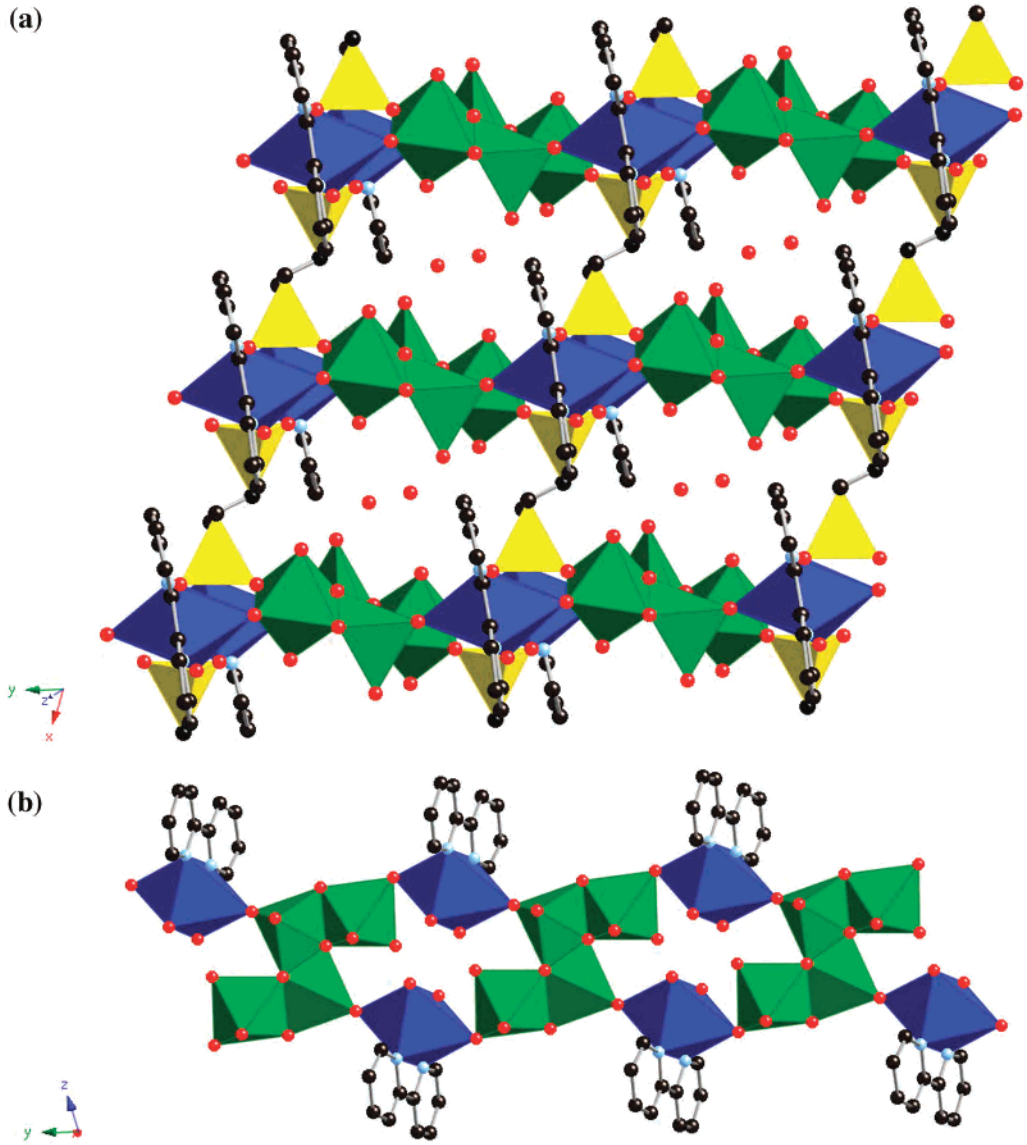

Figure 3. (a) Polyhedral representation of the structure of $[\{Cu(bpy)\}_2(Mo_4O_{12})(H_2O)_2(O_3PCH_2CH_2PO_3)]\cdot 2H_2O$ (**3**·$2H_2O$), parallel to the crystallographic *c* axis. (b) $\{Cu(bpy)(Mo_4O_{12})(H_2O)_2\}_n^{2n+}$ substructure of **3**.

square pyramids are each involved in *cis*-base edge-sharing with the exterior Mo(VI) octahedra. The square pyramidal site is defined in the basal plane by a doubly bridging oxo-group to the octahedral Mo center, two triply bridging oxo-groups to the neighboring square pyramidal center and to the octahedral Mo site, and an oxo-group bridging to the Cu site, while a terminal oxo-group occupies the apical position. The octahedral molybdate exhibits bonding to a terminal oxo-group, a doubly bridging oxo-group to the square pyramidal site, a triply bridging oxo-group to this site, the oxygen donor of a phosphonate ligand, an oxo-group bridging to the copper center, and an aqua ligand. The Cu(II) sites exhibit "4 + 2" distorted octahedral geometry. The four equatorial bonds are to two oxygen donors of diphosphonate ligands and to the nitrogen donors of the chelating bpy ligand, while long axial interactions are formed to molybdate polyhedra of neighboring clusters. Each terminus of the diphosphonate ligand bridges two Cu sites and one Mo center.

The structure may be described as molybdate clusters linked through copper octahedra into one-dimensional chains which are in turn cross-linked by ethylenediphosphonate subunits into a two-dimensional network. The $\{Cu(bpy)(Mo_4O_{12})(H_2O)_2\}^{2+}$ substructure is shown in Figure 3b.

The polyhedral connectivity generates large $\{Mo_8Cu_2P_4O_{12}C_4\}$ rings of 14 polyhedra connects within the layers. The water molecules of crystallization occupy these intralamellar cavities. The bpy ligands project from the surfaces of the layers into the interlamellar spaces and interdigitate with rings from adjacent layers. The structure of **3**·$2H_2O$ is isomorphous with that of the previously described phenanthroline derivative $[\{Cu(phen)\}_2(Mo_4O_{12})(H_2O)_2(O_3PCH_2CH_2PO_3)]\cdot 2H_2O$.[88]

Expansion of the tether length to three in the propylenediphosphonate derivative $[Cu(bpy)(Mo_2O_5)(O_3PCH_2CH_2CH_2PO_3)]$ (**4**) has unanticipated structural consequences. As shown in Figure 4a, the structure of **4** is layered and constructed of binuclear units of face-sharing molybdate

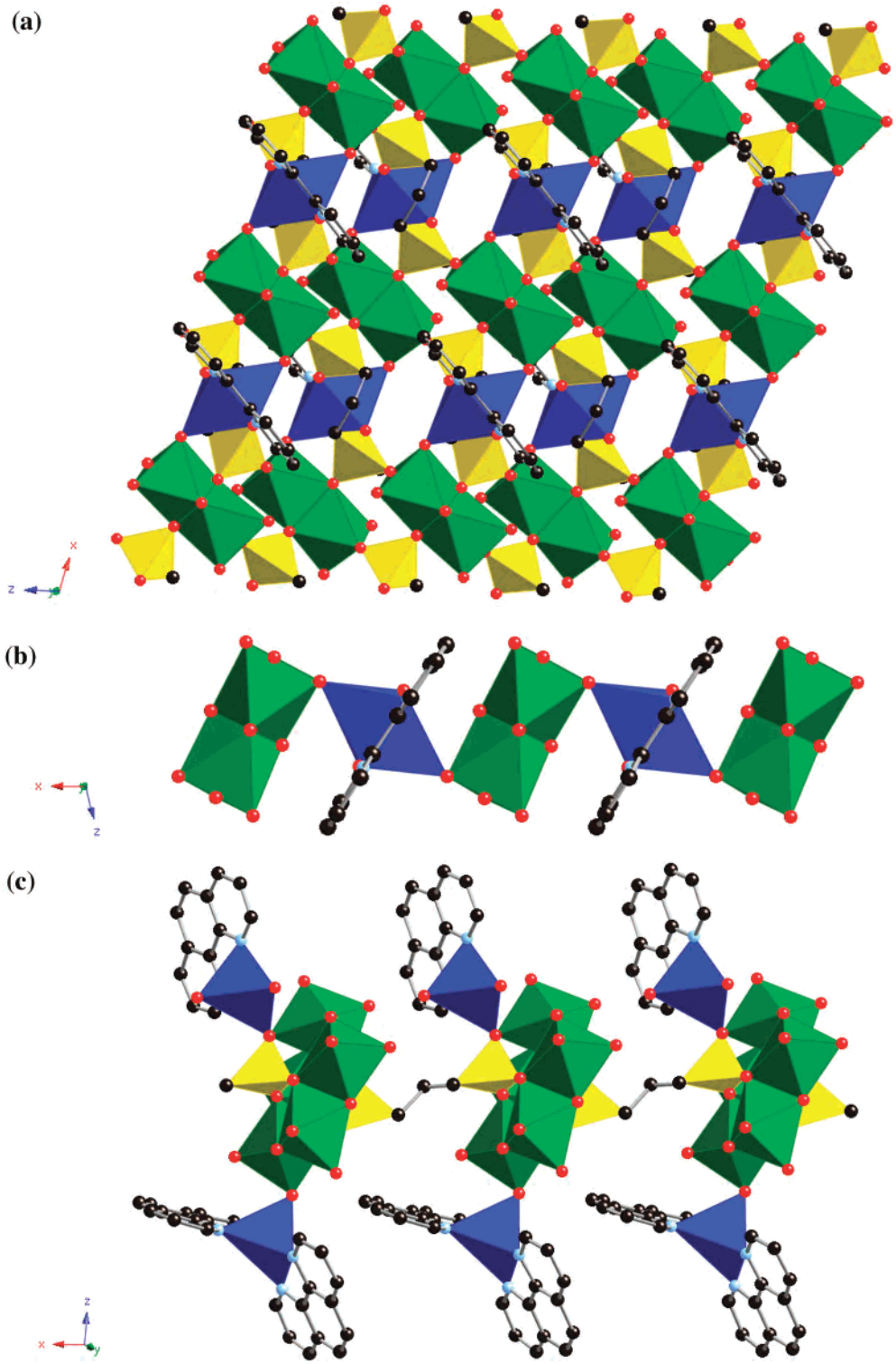

Figure 4. (a) View of the network structure of [Cu(bpy)(Mo_2O_5)($O_3PCH_2CH_2CH_2PO_3$)] (**4**), parallel to the crystallographic *b* axis. (b) Copper molybdate substructure of **4**. (c) View of the structure of [{Cu(phen)(H_2O)$_2$}{Cu(phen)$_2$}(Mo_5O_{15})($O_3PCH_2CH_2CH_2PO_3$)]·2.5H_2O.

octahedra linked through copper octahedra and phosphorus tetrahedra. The Mo geometries are defined by three oxygen donors from diphosphonate ligands, a doubly bridging oxo-group to the second Mo site of the binuclear unit, an oxo-group bridging to a Cu(II) site, and a terminal oxo-group. The Cu(II) site exhibits "4 + 2" six coordination with an equatorial plane defined by the nitrogen donors of the chelating bpy ligand and two oxygen donors from diphosphonate groups; the long axial interactions are with oxo-groups from two neighboring molybdate binuclear units.

The most unusual feature of the structure of **4** is the disposition of the propylenediphosphonate ligand. Two oxygen donors of each phosphorus terminus link to molybdate groups of two neighboring binuclear subunits; consequently, each diphosphonate group bridges four binuclear subunits. Curiously, the remaining oxygen donors are

employed in chelation to a single Cu(II) center, such that the diphosphonate folds to form a most unusual eight-membered {Cu−O−P−C−C−C−P−O−} chelate ring. One consequence of this bonding pattern is to produce a much less open network than that associated with **3**·$2H_2O$, a feature consistent with the absence of water of crystallization within the layers of **4**.

The copper molybdate substructure of **4** $\{Cu(bpy)(Mo_2O_5)\}^{4+}$ is a one-dimensional chain of binuclear molybdate subunits bridged by $\{Cu(bpy)\}^{2+}$ moieties. These chains are connected in turn by the propylenediphosphonate ligands. As shown in Figure 4b, the structure may be alternatively described as a two-dimensional organophosphomolybdate network with $\{Cu(bpy)\}^{2+}$ moieties embedded in the cavities produced by the long propylene tethers of the diphosphonate ligands.

In contrast to the structure of **4**, phenanthroline derivative $[\{Cu(phen)(H_2O)_2\}\{Cu(phen)_2\}(Mo_5O_{15})(O_3PCH_2CH_2CH_2PO_3)]\cdot 2.5H_2O$[88] is constructed from the anticipated phosphomolybdate clusters linked through the propylene tethered phosphonate ligands, as shown in Figure 4c. The structural differences demonstrate the dramatic and unpredictable consequences of minor modifications, even in the nature of the ligand to the secondary metal site. As discussed later, the structure of $[\{Cu(phen)(H_2O)_2\}\{Cu(phen)_2\}(Mo_5O_{15})(O_3PCH_2CH_2CH_2PO_3)]\cdot 2.5H_2O$ is more closely related to that of the butylenediphosphonate derivative **5**·H_2O.

Upon further expansion of the diphosphonate tether in $[\{Cu(bpy)_2\}\{Cu(bpy)(H_2O)\}(Mo_5O_{15})(O_3PCH_2CH_2CH_2CH_2PO_3)]\cdot H_2O$ (**5**·H_2O), incorporation of the anticipated subunit $\{Mo_5O_{15}(O_3PR)_2\}^{4-}$ is finally achieved, as shown in Figure 5. The one-dimensional structure of **5** is constructed from the phosphomolybdate clusters linked through butylene bridges and decorated with corner-sharing Cu(II) square pyramids. The phosphomolybdate clusters consist of a ring of edge- and corner-sharing $\{MoO_6\}$ octahedra capped at either pole by corner-sharing $\{O_3PR\}^{2-}$ groups. The $\{Mo_5O_{15}(O_3PR)_2\}^{4-}$ subunit is structurally identical to those previously reported for the isolated clusters of the types $[Mo_5O_{15}(O_3PX)_2]^{4-}$ (X = OH, OR, R) and $[Mo_5O_{15}(PO_4)_2]$.[6−87,102,103]

Two different Cu(II) moieties decorate the exterior of the molybdate rings. The Cu(1) square pyramid is defined by four nitrogen donors from two chelating bpy ligands in the basal plane and an apical oxo-group bridging to an $\{MoO_6\}$ octahedron. The Cu(2) site exhibits bonding to two nitrogen donors from a bpy ligand, an oxygen donor from a doubly bridging phosphonate ligand and an aqua ligand in the basal plane, with an oxo-group bridging to a molybdenum site in the apical position.

While the structure of **5** is analogous to that of $[\{Cu(phen)(H_2O)_2\}\{Cu(phen)_2\}(Mo_5O_{15})\ (O_3PCH_2CH_2CH_2PO_3)]\cdot 2.5H_2O$, the details of the connectivities of the copper subunits to the clusters are not identical, as shown in Figure 5b. Thus, the copper site featuring a single bpy chelate in **5** is bonded to a single aqua ligand and shares an edge with a molybdenum site of the ring, while the similar copper site of the phenanthroline derivative is bonded to two aqua ligands and has a single corner-sharing interaction with the cluster.

The structural differences between the bipyridine derivatives **1**−**5** and the previously reported phenanthroline derivatives encouraged us to prepare a third series of materials of the molybdenum oxide/Cu/diphosphonate/organoimine family, where the ligand to the secondary metal Cu is terpyridine. It was anticipated that the increased denticity of the ligand would constrain the geometry at the copper center and limit the connectivity and bridging possibilities between the cluster sites. As discussed below, this rationale proved somewhat naive.

The unanticipated structural consequences of replacing bpy by terpyridine are demonstrated by the structure of $[Cu(terpy)(Mo_2O_5)(O_3PCH_2PO_3)]$ (**6**), shown in Figure 6. The two-dimensional structure of **6** is constructed from binuclear units of edge-sharing $\{MoO_6\}$ octahedra linked into a one-dimensional phosphomolybdate chain by the methylenediphosphonate ligand which is connected into a two-dimensional network by binuclear subunits of edge-sharing Cu(II) square pyramids. The six coordinate Mo(VI) sites exhibit two *cis*-terminal oxo-groups, a bridging oxo-group between Mo sites and three oxygen donors from two methylenediphosphonate groups. Each methylenediphosphonate ligand spans a binuclear molybdate subunit, sharing two vertices from one phosphorus terminus and one from the second, so as to chelate and bridge both Mo sites of the subunit. Two of the remaining oxygen donors bridge to adjacent molybdate binuclear units, while the third oxygen bridges the copper sites of a binuclear copper subunit. Consequently, each methylenediphosphonate ligand links three molybdate centers and one copper subunit.

The Cu(II) site exhibits "4 + 1" square pyramidal geometry with three nitrogen donors of a terpy ligand and an oxygen donor of a methylenediphosphonate in the basal plane and the apical position occupied by the oxygen from a second diphosphonate ligand. The copper sites of the binuclear unit share an axial/basal edge defined by the oxygen donors at the vertices. In contrast to all the previously described structures of this type, the Cu polyhedra do not share corners or edges with the Mo polyhedra. The structure can thus be described as phosphomolybdate ribbons linked by binuclear Cu subunits into a two-dimensional network.

The connectivity pattern produces twelve polyhedral connects or 24 membered $\{Mo_4Cu_2P_6O_{12}\}$ rings. The terpyridyl ligands project into these intralamellar cavities. Consequently, there is no water of crystallization associated with the layer cavities as in **2**·H_2O, where the reduced steric requirements leave the cavities unencumbered.

The network structure of **6** contrasts with the one-dimensional structures of **1** and $[Cu(phen)(Mo_2O_5)(O_3PCH_2PO_3)]$. Furthermore, while the structure of **2**·$2H_2O$ is also two-dimensional, the phosphomolybdate substructure itself is two-dimensional in contrast to the one-dimensional phosphomolybdate substructure of **6**. In common with other

(102) Hedman, B. *Acta Chem. Scand.* **1977**, *27*, 3335.
(103) Strandberg, R. *Acta Chem. Scand.* **1973**, *27*, 1004.

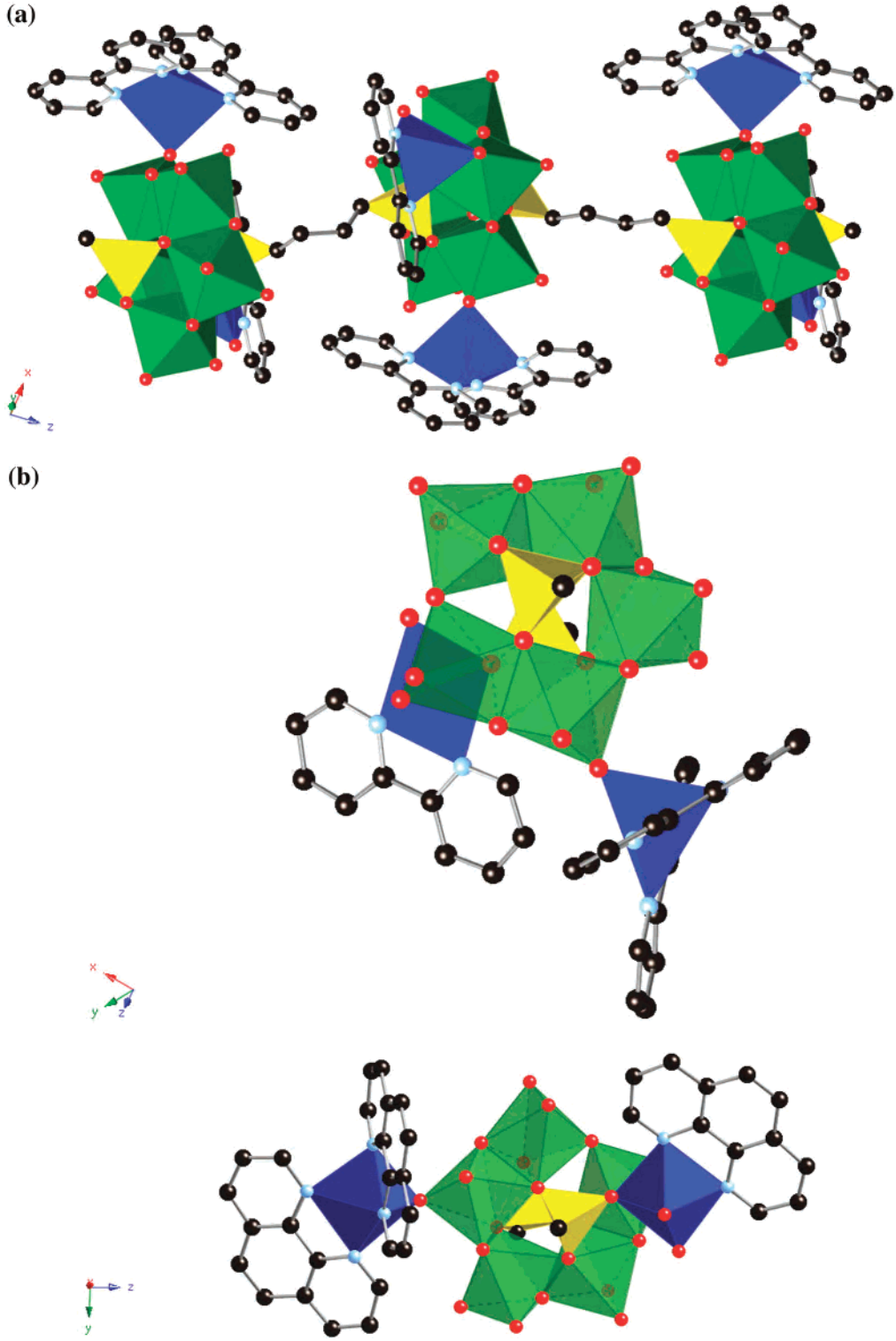

Figure 5. (a) Polyhedral representation of the one-dimensional structure of $[\{Cu(bpy)_2\}\{Cu(bpy)(H_2O)\}(Mo_5O_{15})(O_3PCH_2CH_2CH_2CH_2PO_3)]\cdot H_2O$ (**5**·H_2O), viewed parallel to the crystallographic *b* axis. (b) Copper unit-cluster geometries of **5** and $[\{Cu(phen)(H_2O)_2\}\{Cu(phen)_2\}(Mo_5O_{15})(O_3PCH_2CH_2CH_2PO_3)]\cdot 2.5H_2O$.

structures of the family, the copper sites of **2** link to the molybdate subunits, unlike the binuclear copper sites of **6**.

The expansion of the tether length in the ethylenediphosphonate derivative $[\{Cu(terpy)(H_2O)\}_2(Mo_5O_{15})(O_3PCH_2CH_2PO_3)]\cdot 3H_2O$ (**7**·$3H_2O$) results in a structure constructed from the $\{Mo_5O_{15}(O_3P-)_2\}^{4-}$ cluster building blocks, linked into a chain through the ethylene spaces of the diphosphonate and decorated with $\{Cu(terpy)\}^{2+}$ subunits, as shown in Figure 7. The geometry of the phosphomolybdate cluster component is unexceptional and may be compared to the cluster moieties of $[\{Cu(bpy)_2\}\{Cu(bpy)(H_2O)\}(Mo_5O_{15})(O_3PCH_2CH_2CH_2PO_3)]\cdot H_2O$ (**5**·H_2O) and of $[\{Cu(phen)_2\}\{Cu(phen)(H_2O)_2(Mo_5O_{15})(O_3PCH_2CH_2CH_2PO_3)]\cdot 2.5H_2O$. However, the details of attachment of the $\{Cu(terpy)\}^{2+}$ subunits

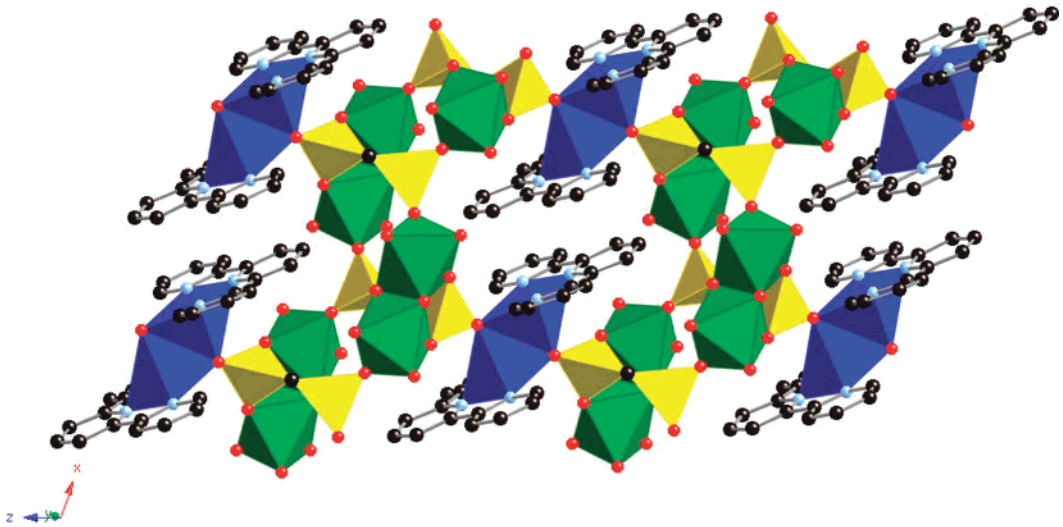

Figure 6. View of the two-dimensional structure of [Cu(terpy)(Mo_2O_5)($O_3PCH_2PO_3$)] (**6**), shown parallel to the crystallographic *b* axis.

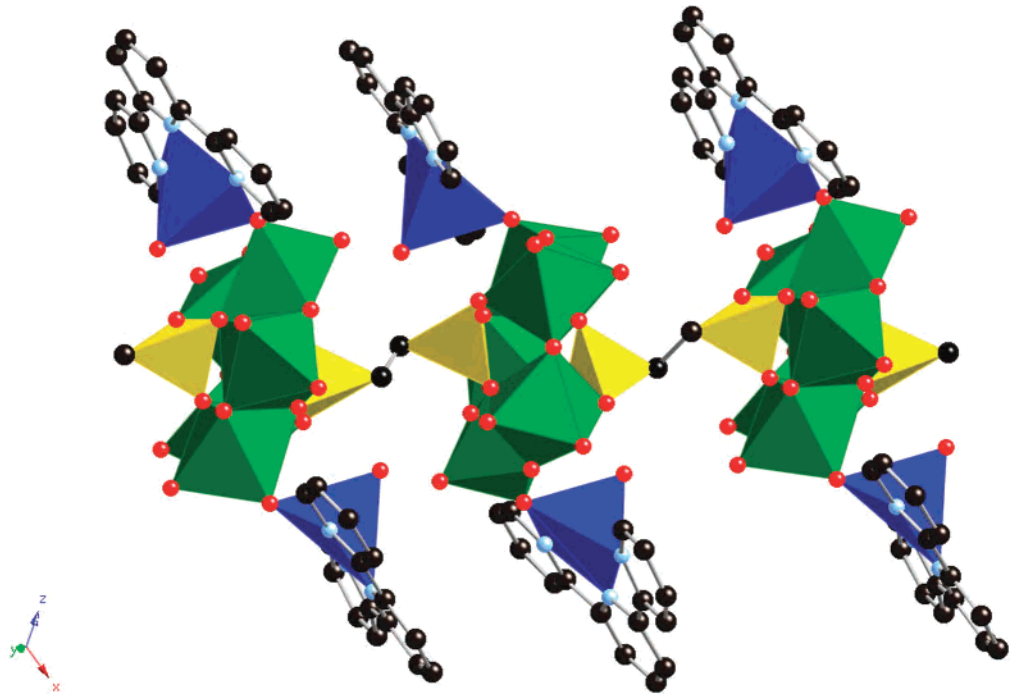

Figure 7. View of the one-dimensional structure of [{Cu(terpy)(H_2O)}$_2$(Mo_5O_{15})($O_3PCH_2CH_2PO_3$)]·7H_2O (**7**·3H_2O), parallel to the *b* axis.

in **7** is distinct from those observed for the latter two structures. The Cu(II) square planar geometry of **7** is defined by three nitrogen donors of the terpy ligand and a bridging oxo-group in the basal plane and by an aqua ligand in the apical position. Thus, each Cu(II) polyhedron shares a single vertex with the molybdate ring.

While the structure of [{Cu(terpy)}$_2$(Mo_5O_{15})($O_3PCH_2CH_2CH_2PO_3$)] (**8**) is also based on the common {Mo_5O_{15}(O_3P−)$_2$}$^{4-}$ cluster building block, the material is two-dimensional in contrast to the chain structures of **5**, **7**·3H_2O, and [{Cu(phen)$_2$}{Cu(phen)(H_2O)$_2$}(Mo_5O_{15})($O_3PCH_2CH_2CH_2PO_3$)], the other representatives of this structural motif. As shown in Figure 8, the structure consists of organodiphosphonate−pentamolybdate chains {Mo_5O_{15}}($O_5PCH_2CH_2CH_2PO_3$)}$_n^{4n-}$ linked through {Cu(terpy)}$^{2+}$ square pyramids into a two-dimensional network. The phosphomolybdate substructure is analogous to those of **5** and **7**. The Cu(II) square pyramidal subunits exhibit a basal plane defined by three nitrogen donors of the terpy ligand and a bridging oxo-group from a molybdate site and an apical site occupied by a second bridging oxo-group. Each {Cu(terpy)}$^{2+}$ bridges phosphomolybdate clusters from two adjacent {(Mo_5O_{15})($O_3PCH_2CH_2CH_2PO_3$)}$_n^{4n-}$ chains. Consequently, the structure may be alternatively described as copper molybdate chains {$Cu_2Mo_5O_{15}$}$_n^{4n+}$ linked through propylenediphosphonate ligands into a two-dimensional network. The cross-linking {$Cu_2Mo_5O_{15}$}$_n^{4n+}$ and {(Mo_5O_{15})($O_3PCH_2CH_2CH_2PO_3$)}$_n^{4n-}$ chains intersect at an angle of ∼78°.

The structures of this study exhibit a remarkable range of component substructures and polyhedral connectivities. To date, the family of materials of the type oxomolybdate/O_3P-

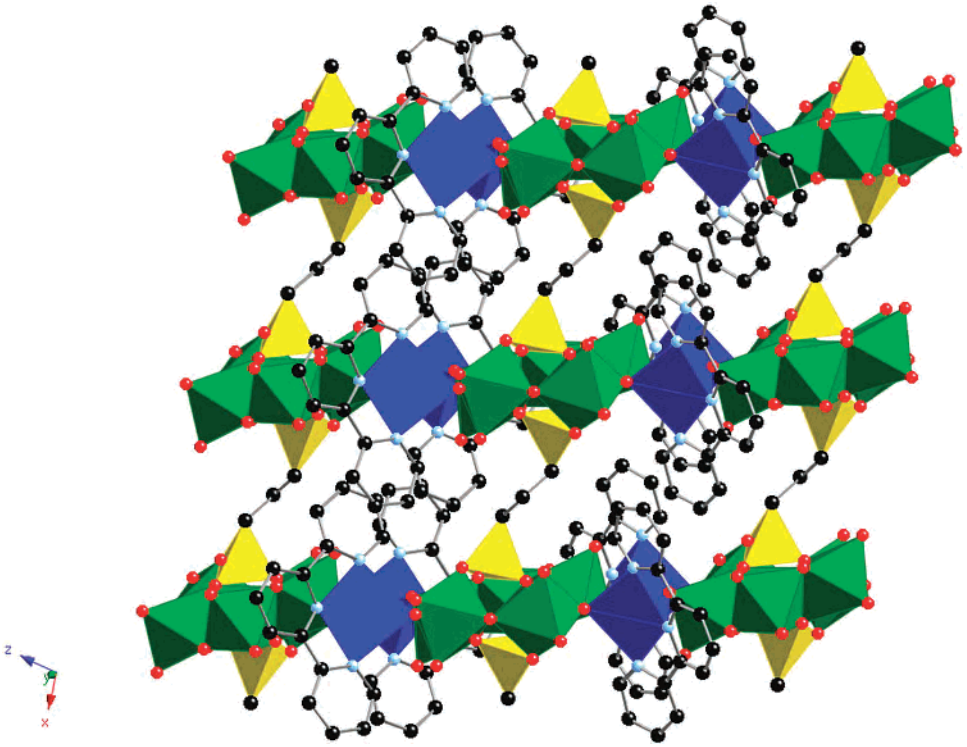

Figure 8. Polyhedral representation of the two-dimensional structure of [{Cu(terpy)}$_2$ (Mo_5O_{15})($O_3PCH_2CH_2CH_2PO_3$)] (**8**), parallel to the *b* axis.

$(CH_2)_nPO_3^{4-}$/Cu(II)/organoimine is represented by $n = 1-4$ and by the organoimine ligands 2,2′-bipyridine, *o*-phenanthroline, 2,2′:6′,2″-terpyridine, and tetra(4-pyridyl)pyrazine. While the $\{(Mo_5O_{15})(O_3P-)_2\}^{4-}$ cluster is a recurring motif, it is not ubiquitous, as manifested in the structural summary of Table 2.

The structural summary evokes a number of observations. While a significant database has been compiled for this unusually fruitful family of materials, it is clear that the set of compounds is not exhaustive in view of the structural variability associated with the constituent building blocks. This latter point is reflected in the different coordination geometries accessible for Mo(VI), including tetrahedral, square pyramidal, and octahedral, as well as the aggregation of molybdenum polyhedra into larger oligomers. Furthermore, the diphosphonate ligand may adopt a variety of coordination modes with respect to the molybdate subunit and the secondary metal component, which also enjoys considerable latitude in coordination geometry and polyhedral connectivity to the molybdophosphonate substructure. Finally, coordinated water molecules are often constituents of both the molybdenum and the copper coordination sphere in phases which have been prepared hydrothermally at moderate temperature. Thus, it may be anticipated that for a given combination of organoimine coligand to the Cu(II) subunit and organodiphosphonate linker more than one phase may be accessible by appropriate manipulation of the hydrothermal conditions. Hydrothermal parameter space, which includes stoichiometries, pH, temperature, and fill volume, is vast, and even minor variations can result in the isolation of new metastable phases. This point is illustrated by the isolation of two phases **1** and **2**·H_2O for methylenediphosphonate and 2,2′-bipyridine combination of ligands. It is likely that other combinations of organodiphosphonates and 2,2′-bipyridine or terpyridine will also yield more than one phase as the hydrothermal conditions are more fully explored.

The most apparent structural trend is observed for the methylenediphosphonate derivatives **1**, **2**·H_2O, and **6**. The methylene spacer does not allow extension of the diphosphonate ligand to link two discrete substructural motifs, but rather constrains the ligand to act as a chelate forming six-membered {M−O−P−C−P−O−} rings. However, within this limitation, there is considerable flexibility as the methylenediphosphonate may chelate either the Mo or the Cu sites and may establish a variety of connectivity patterns with the remaining oxygen donors, an observation manifest in the distinct structures of **1**, **2**·H_2O, and **6**.

The copper coordination geometry is also variable in this structural set. While mononuclear square pyramidal sites are most common, mononuclear six coordinate and even binuclear sites are also incorporated into the overall architectures. Water coordination is also evident, often giving rise to more than one geometric type in a material, as illustrated by **5**·H_2O, [{Cu(phen)}$_2${Cu(phen)(H_2O)$_2$}(Mo_5O_{15})($O_3PCH_2CH_2CH_2PO_3$)]·2.5H_2O, and [{Cu_2(tpypyz)(H_2O)$_2$}(Mo_5O_{15})($O_3PCH_2CH_2PO_3$)]·5.5H_2O.

Although the syntheses were carried out under conditions favoring the formation of $\{(Mo_5O_{15})(O_3PR)_2\}^{4-}$ clusters, a variety of molybdenum substructures are observed, including discrete {MoO_6} octahedra, binuclear, tetranuclear, and pentanuclear units. While the $\{(Mo_5O_{15})(O_3P-)_2\}^{4-}$ motif appears in 5 of 12 structures, the overall architecture may be one-dimensional (**5**·H_2O, **7**·3H_2O, and [{Cu(phen)$_2$}{Cu(phen)(H_2O)$_2$}(Mo_5O_{15})($O_3PCH_2CH_2$ CH_2PO_3)]·2.5H_2O) or two-dimensional **8** and [{Cu_2(tpypyz)(H_2O)$_2$}(Mo_5O_{15})(O_3-

Table 2. Summary of Structural Characteristics for Materials of the Oxomolybdate/Diphosphonate/Cu(II)/Organoimine Family

compound	overall dimensionality	Cu(II) component structure	molybdate substructure	copper molybdate substructure	phosphomolybdate substructure
$[Cu(bpy)(MoO_2)(H_2O)(O_3PCH_2PO_3)]$ (**1**)	1-D	$\{CuN_2O_3\}$ square pyramid	isolated $\{MoO_6\}$ octahedra	binuclear unit	$\{MoO_2(H_2O)(O_3PCH_2PO_3)\}_n^{2n-}$ chain
$[Cu(bpy)(Mo_2O_5)(H_2O)(O_3PCH_2PO_3)]\cdot H_2$ (**2**·H_2O)	2-D	$\{CuN_2O_3\}$ square pyramid	binuclear unit of edge-sharing octahedra	trinuclear unit	$\{(Mo_2O_5)(H_2O)(O_3PCH_2PO_3)\}_n^{2n-}$ network
$[\{Cu(bpy)\}_2(Mo_4O_{12})(H_2O)_2(O_3PCH_2CH_2PO_3)]\cdot 2H_2O$ (**3**·$2H_2O$)	2-D	$\{CuN_2O_4\}$, "4 + 2" octahedron	tetranuclear cluster of edge-sharing octahedra and square pyramids	$\{Cu(bpy)(Mo_4O_{12})(H_2O)_2\}_n^{4n-}$ chain	$\{(Mo_4O_{12})(H_2O)_2(O_3PCH_2CH_2PO_3)\}_n^{4n-}$ network
$[Cu(bpy)(Mo_2O_5)(O_3PCH_2CH_2CH_2PO_3)]$ (**4**)	2-D	$\{CuN_2O_4\}$, "4 + 2" octahedron	binuclear cluster of face-sharing octahedra	$\{Cu(bpy)(Mo_2O_5)\}_n^{4n+}$ chain	$\{(Mo_2O_5)(O_3PCH_2CH_2CH_2PO_3)\}_n^{2n-}$ network
$[\{Cu(bpy)_2\}\{Cu(bpy)(H_2O)\}(Mo_5O_{15})(O_3PCH_2CH_2CH_2CH_2PO_3)]\cdot H_2O$ (**5**·H_2O)	1-D	$\{CuN_4O\}$ and $\{Cu_2O_3\}$ square pyramids	$\{Mo_5O_{15}\}$ ring of edge- and corner-sharing octahedra	$\{Cu_2(bpy)_3(H_2O)(Mo_5O_{15})\}^{4+}$ cluster	$\{(Mo_5O_{15})(O_3PCH_2CH_2CH_2CH_2PO_3)\}_n^{4n-}$ chain
$[Cu(phen)(Mo_2O_5)(H_2O)(O_3PCH_2PO_3)]$	1-D	$\{CuN_2O_3\}$ square pyramid	binuclear unit of edge-sharing octahedra	trinuclear unit	$\{(Mo_2O_5)(O_3PCH_2PO_3)\}_n^{2n-}$ chain
$[\{Cu(phen)\}_2(Mo_4O_{12})(H_2O)_2(O_3PCH_2CH_2PO_3)]\cdot 2H_2O$	2-D	$\{CuN_2O_3\}$ square pyramid	tetranuclear unit of edge- and corner-sharing octahedra and square pyramids	$\{Cu_2(phen)_2(Mo_4O_{12})\}_n^{4n+}$ chain	$\{(Mo_4O_{12})(O_3PCH_2CH_2PO_3)\}_n^{4n-}$ chain
$[\{Cu(phen)_2\}\{Cu(phen)(H_2O)_2\}(Mo_5O_{15})(O_3PCH_2CH_2CH_2PO_3)]\cdot 2\cdot 5H_2O$	1-D	$\{CuN_4O\}$ and $\{CuN_2O_3\}$ square pyramids	$\{Mo_5O_{15}\}$ ring of edge- and corner-sharing octahedra	$\{Cu_2(phen)_3(H_2O)_2(Mo_5O_{15})\}^{4+}$ cluster	$\{(Mo_5O_{15})(O_3PCH_2CH_2CH_2PO_3)\}_n^{4n-}$ chain
$[Cu(terpy)(Mo_2O_5)(O_3PCH_2PO_3)]$ (**6**)	2-D	binuclear unit of edge-sharing square pyramids	binuclear unit of edge-sharing octahedra	no connectivity between Cu and Mo polyhedra	$\{(Mo_2O_5)(O_3PCH_2PO_3)\}_n^{4n-}$ chain
$[\{Cu(terpy)(H_2O)\}_2(Mo_5O_{15})(O_3PCH_2CH_2PO_3)]\cdot 3H_2O$ (**7**·$3H_2O$)	1-D	$\{CuN_3O_2\}$ square pyramid	$\{Mo_5O_{15}\}$ ring of edge- and corner-sharing octahedra	$\{Cu_2(terpy)_2(H_2O)_2(Mo_5O_{15})\}^{4+}$ cluster	$\{(Mo_5O_{15})(O_3PCH_2CH_2PO_3)\}_n^{2n-}$ chain
$[\{Cu(terpy)\}_2(Mo_5O_{15})(O_3PCH_2CH_2CH_2PO_3)]$ (**8**)	2-D	$\{CuN_3O_2\}$ square pyramid	$\{Mo_5O_{15}\}$ ring of edge- and corner-sharing octahedra	$\{Cu_2(terpy)_2(Mo_5O_{15})\}_n^{4n+}$ chain	$\{(Mo_5O_{15})(O_3PCH_2CH_2PO_3)\}_n^{4n-}$ chain
$[\{Cu_2(tpypyz)(H_2O)_2\}(Mo_5O_{15})(O_3PCH_2CH_2PO_3)]\cdot 5\cdot 5H_2O$	2-D	$\{CuN_3O_2\}$ square pyramid and $\{CuN_3O_3\}$ octahedron	$\{Mo_5O_{15}\}$ ring of edge- and corner-sharing octahedra	$\{Cu_2(terpy)(H_2O)_2(Mo_5O_{15})\}_n^{4n-}$ chains	$\{(Mo_5O_{15})(O_3PCH_2CH_2PO_3)\}_n^{4n-}$ chains

$PCH_2CH_2PO_3)]\cdot 5.5H_2O$ (tpypyz = tetra-4-pyridylpyrazine). The cluster core is associated exclusively with phosphomolybdate chain substructures. While the cluster motif spans diphosphonates $\{O_3P(CH_2)_nPO_3\}^{4-}$ for $n = 2$, 3, and 4, its presence is also contingent on the organoimine coligand. For example, the cluster substructure is observed for the propylenediphosphonate derivatives $[\{Cu(phen)_2\}\{Cu(phen)(H_2O)_2\}(Mo_5O_{15})(O_3PCH_2CH_2CH_2PO_3)]\cdot 2.5H_2O$ and **8** but is absent in the structure of **4**. Similarly, the cluster substructure is present for the ethylenediphosphonate series in the case of **7**·$3H_2O$ and $[\{Cu_2(tpypyz)(H_2O)_2\}(Mo_5O_{15})(O_3PCH_2CH_2PO_3)]\cdot 5.5H_2O$ but absent for $[\{Cu(phen)\}_2(Mo_4O_{12})(H_2O)_2(O_3PCH_2CH_2PO_3)]\cdot 2H_2O$.

While four phases exhibit binuclear molybdate building blocks, three involve edge-sharing octahedra, but the fourth is an unusual example of a face-sharing binuclear unit. A curious feature of these structures is that two exhibit two-dimensional phosphomolybdate substructures (**2**·H_2O and **4**), while two contain one-dimensional phosphomolybdate components, $[Cu(phen)(Mo_2O_5)(H_2O)(O_3PCH_2PO_3)]$ and **6**.

The two phases incorporating the tetranuclear molybdate core, **3**·$2H_2O$ and $[\{Cu(phen)\}_2(Mo_4O_{12})(H_2O)_2(O_3PCH_2CH_2PO_3)]\cdot 2H_2O$, are the only isomorphous pairs to be revealed to date. This may suggest that, under appropriate conditions, isomorphous phenanthroline derivatives of **1**, **2**, **4**, and **5** may be accessible.

The thermal decomposition profile of the compound **3**·$2H_2O$ is representative of the series. The water loss begins almost immediately on heating, indicative of loosely held water of crystallization in the interlamellar space and intralamellar cavities of **3**·$2H_2O$. The first weight of ~6.0% to 220 °C indicates that even the bulk of the coordinated water molecules are lost at 220 °C (calculated weight loss for $4H_2O$ molecules: 5.64%). This is followed by ligand loss between 350 and 575 °C to produce an amorphous residue. For compounds **1**, **2**·H_2O, **3**·$2H_2O$, **5**·H_2O, and **7**·$3H_2O$, a similar pattern is observed: water loss below 220 °C, followed by ligand decomposition in the 350−550 °C range. For the compounds **4**, **6**, and **8** which contain no ligated or crystallization water, the only weight losses

occur in the 350−550 °C range, corresponding to ligand loss.

Conclusions

A series of novel and complex structure types of the oxomolybdate/diphosphonate/Cu(II)/organoimine family have been isolated from hydrothermal media and structurally characterized. The results reinforce the observation that hydrothermal chemistry offers an effective synthetic tool for the isolation of composite organic−inorganic materials. It is also clear that organic ligands with specific geometric requirements may be introduced as structural components of materials. Bridging ligands may be used to propagate the architecture about a metal site, while the steric influences of coligands to a secondary metal site may be exploited to dictate the dimensionality of the product. Manipulation of the microstructure of the solid is thus achieved by tuning the coordination influences of the metal to the geometric requirements of the ligand.

It is noteworthy that the materials of this study require the presence of the secondary metal/ligand coordination complex cation for isolation. This structural component serves not only a space-filling and charge-compensating role but is also intimately involved in structural propagation in one or two dimensions.

While it is now evident that organic components may be introduced into the synthesis of solid-state inorganic materials in order to manipulate the coordination chemistry of the metal and consequently the structure of the material, designed extended structures remain elusive in the sense of predictability of the final structure. However, this observation reflects the compositional and structural versatility of inorganic materials and should be considered an opportunity for development rather than an occasion for lamentation. The subtle interplay of metal oxidation states, coordination preferences, polyhedral variability, ligand donor groups, types, and orientations, spatial extension, and steric constraints provides a limitless set of construction components for solid-state materials. As the products of empirical observations are elucidated, the structure−function relationships of such components will begin to emerge and to provide further guidelines for synthetic methodologies.

Acknowledgment. This work was supported by a grant from the National Science Foundation (CHE 9987471).

Supporting Information Available: ORTEP figures showing the labeling scheme and 50% probability ellipsoids for **1**−**8**. Listings of crystal data and collection parameters, atomic positional parameters, anisotropic thermal parameters, and complete listings of bond lengths and angles for **1**−**8** in CIF format. This material is available free of charge via the Internet at http://pubs.acs.org.

IC011124V